universität wien

MASTERARBEIT / MASTER'S THESIS

Titel der Masterarbeit / Title of the Master's Thesis

„TAT-SMN1-mediated protein delivery into mammalian cells“

verfasst von / submitted by

Azra Kurtović, BSc

angestrebter akademischer Grad / in partial fulfilment of the requirements for the degree of

Master of Science (MSc)

Wien, 2018 / Vienna 2018

Studienkennzahl lt. Studienblatt / degree programme code as it appears on the student record sheet:	A 066 834
Studienrichtung lt. Studienblatt / degree programme as it appears on the student record sheet:	Masterstudium Molekulare Biologie
Betreut von / Supervisor:	Ass. Prof. Priv. Doz. Dr. Franco Laccone

Danksagung

Ich möchte mich bei allen Personen bedanken, die mich beim Schreiben meiner Masterarbeit unterstützt haben, allen voran meiner Familie, die mir Kraft spendend zur Seite gestanden ist, Freunden und Kollegen, denen ich Anregungen zu verdanken habe, nicht zuletzt aber Mag. Dr. Hannes Steinkellner, der diese Arbeit betreut und mir immer wieder wertvolles Feedback hat zukommen lassen. Ebenso gilt mein Dank Ass. Prof. Priv. Doz. Dr. Franco Laccone für die Ermöglichung meiner Arbeit in seiner Arbeitsgruppe. Des Weiteren bedanke ich mich bei Dr. Alexander Beribisky für seine Anregungen und Korrekturarbeit. Ich bedanke mich auch bei all jenen, die mir durch Tipps und Anmerkungen weitergeholfen haben; auch wenn sie nicht namentlich genannt sind – weil ihrer doch viele sind – so bin ich mir sehr wohl dessen bewusst, dass ich diese Arbeit nicht oder nicht so gut ohne ihre Hilfe bewältigen hätte können, und hoffe, mich bei Gelegenheit einmal gebührend bei ihnen revanchieren zu können. Eine Person, die in dieser Aufzählung nicht fehlen darf, ist Ryan Hennawi. Ryan, ich bin dir unendlich dankbar für deine bedingungslose Unterstützung.

Table of Contents

1. Introduction

1.1. Spinal muscular atrophy

Spinal muscular atrophy (SMA) is an autosomal recessive neuromuscular disease. This disease is characterized by degenerative loss of alpha motor neurons in the brain stem and spinal cord. This loss leads to general muscular weakness and atrophy. SMA affects 1 in 6.000 to 1 in 10.000 live births and has a carrier frequency of 1:40 – 1:60 (Nurputra et al., 2013; Prior et al., 2010). The deletion associated with SMA onset has been localized to chromosome 5q13 (Lefebvre et al., 1995).

SMA is a neuromuscular disease, so a basic understanding of the neuromuscular system is necessary to explain the condition.

1.1.1. The neuromuscular system – Motor neurons and neuromuscular junctions

Motor neurons are part of the central nervous system (CNS). They are categorized into two main groups: upper motor neurons and lower motor neurons. Upper motor neurons are found in the cerebral cortex, while lower motor neurons are arranged in the brainstem and spinal cord. A lesion in the upper motor neurons leads to uncontrolled movement and spasticity, whereas a lesion of lower motor neurons results in paralysis (Stifani, 2014). Muscle contraction is a complicated process, which requires different motor neuron subtypes. Lower motor neurons can be further sub-divided into three groups: alpha (α), beta (β), and gamma (γ) motor neurons. This distinction is made based on the type of muscle fiber of which each type of neuron is composed. α-motor neurons are responsible for muscle contraction and skeleton movement. γ-motor neurons play a role in motor control, and they are responsible for the sensitivity of muscle spindles to stretching; β-neurons excite intra- and extrafusal fiber (Kanning et al., 2010).

Neuromuscular junctions (NMJs) are formed by motor neurons, muscle fibers and Schwann cells. Motor neurons branch into various nerve endings and are part of the presynaptic region of the NMJ. These nerve endings overlay the muscle fiber. The nerve termini contain a high number of acetylcholine (ACh) containing vesicles. The NMJ transduces electrical impulses from the motor neuron to the muscle fibers. This action potential leads to the release of ACh from the presynaptic membrane. The released ACh subsequently binds to ACh receptors on the postsynaptic membrane. This binding triggers Na^+ influx and electrical depolarization,

which produces an Endplate potential (EPP) that excites muscle fibers (Deschenes et al., 1994).

It has been observed that SMA also plays a role in NMJ condition. NMJs in an SMA mouse model have been found to show abnormalities (Hamilton & Gillingwater, 2013; Kariya et al., 2008; Nurputra et al., 2013). As such, SMA is thought to lead to the degeneration of motor neurons in the spinal cord, which manifests in muscle weakness.

1.1.2. The genetic pathogenesis of Spinal muscular atrophy

SMA is linked to chromosome 5q13. Both the *survival motor neuron 1 (SMN1)* gene and the *survival motor neuron 2 (SMN2)* gene are located on 5q13. *SMN1* and *SMN2* differ in only five nucleotides. A C/T base pair exchange in position +6 on exon 7 leads to alternative splicing and the loss of exon 7 in *SMN2* **(Figure 1).** Only about 10% of *SMN2* transcripts possess exon 7 (Jodelka et al., 2010; C. L. Lorson et al., 1999). The truncated SMN2, also called $SMN^{\Delta 7}$ protein, shows a reduced stability in neurons (Vitte et al., 2007). In two-hybrid testing, the $SMN^{\Delta 7}$ protein has shown a lesser ability to self-associate. $SMN^{\Delta 7}$ is also less stable than full-length SMN (C. L. Lorson et al., 1999; Christian L. Lorson et al., 1998). Cho and Dreyfuss have shown that $SMN^{\Delta 7}$ has a *c*-terminal degradation signal, which links it to proteasomal degradation (Cho & Dreyfuss, 2010).

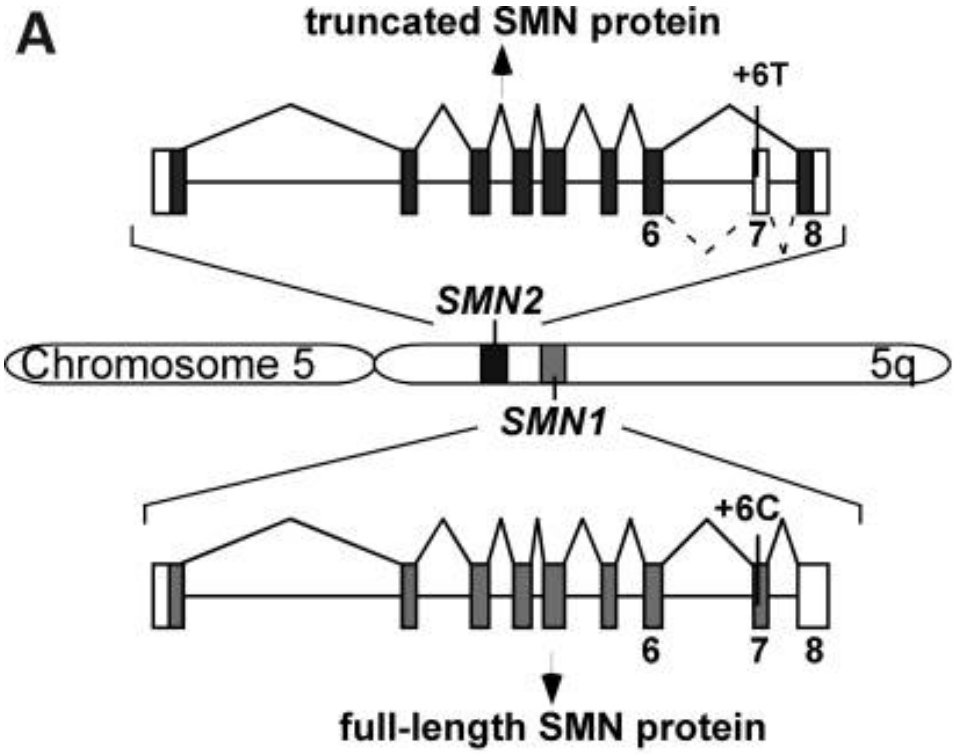

Figure 1: The SMN protein. The full-length SMN protein and the truncated SMN, SMNΔ7, protein (taken from (Jodelka et al., 2010).

1.1.3. The survival motor neuron protein

The *SMN* gene encodes a ubiquitously expressed, 294-amino-acid, 38 kDa SMN protein. The protein is localized in the nucleus and in the cytoplasm (Lefebvre et al., 1997; Q. Liu & Dreyfuss, 1996). A 30-amino-acid region spanning residues 249-278 has been shown to be responsible for SMN1 self-oligomerization as mutations in the aforementioned region lead to the disruption of this process (Christian L. Lorson et al., 1998). SMN is found in nuclear structures called gemins, where it colocalizes with gemin proteins, derived from the term "Gemini (Twins) of coiled bodies". Coiled bodies are a previously discovered nuclear structure (Q. Liu et al., 1996), and SMN self-oligomerizes and builds a stable complex with gemin proteins. Gemins 2–8 are found to be part of this survival motor neuron complex (SMN complex) (Gubitz et al., 2004). UNR-interacting protein (unrip), another component of the SMN complex, may play a role in its localization (Carissimi et al., 2005). In order to understand SMA, it is important to gain a deeper insight into the SMN protein and its functions.

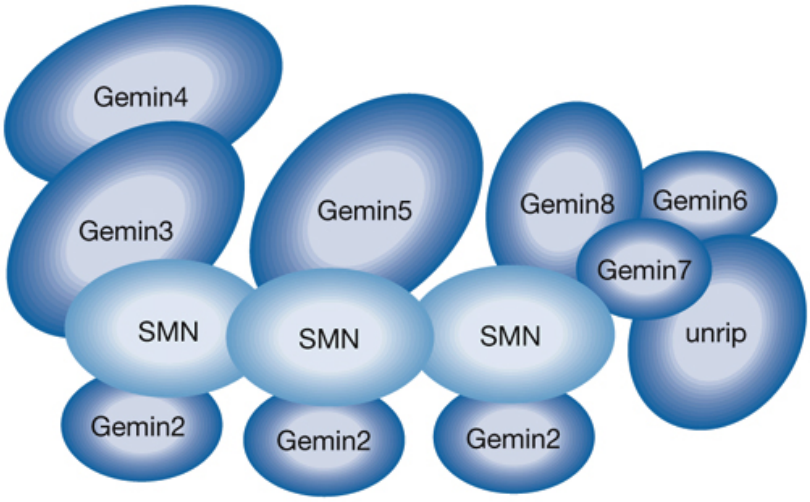

Figure 2: The SMN-complex. The SMN complex is composed of SMN and Gemin2-8 and unrip (taken from (Pellizzoni, 2007).

1.1.4. Function of the survival motor neuron protein

The SMN complex is found to play a role in the assembly of spliceosomal small nuclear ribonucleoproteins (snRNPs). SnRNPs are a component of the splicing apparatus. The SMN complex interacts with SM proteins and SM-like proteins (Fischer et al.; Gubitz et al., 2004). Pellizzoni et al. suggest that the role of the SMN complex is to ensure that only intended RNAs interact with their SM protein binding partner (Pellizzoni et al., 2002). It was demonstrated that there is a correlation between the amount of SMN and snRNPs assembly and that snRNP assembly was decreased in SMA patients. In addition, mouse experiments showed a correlation between disease severity and snRNP assembly impairment (Gabanella et al., 2007; Wan et al., 2005).

Considering that SMN plays a role in pre–messenger-RNA (mRNA) splicing, all tissues should be affected, not just motor neurons. There are two theories that explain the tissue-specific characteristics of SMA. The first is that there is a possibility that motor neurons are more sensitive to the loss of SMN. This might be due the change of splicing of one particular RNA. The other theory is that SMN may have a motor neuron specific function (Monani, 2005). Fan & Simard observed that SMN accumulated in growth cones and NMJs during neuronal differentiation (Fan & Simard, 2002). Zhang et al. have shown that SMN is organized in granules that are localized in growth cones and neurites. They also observed that

SMN granules move bidirectionally and that microtubules and microfilaments are involved in the movement process. They furthermore tested the role of exon 7 in SMN localization. Their findings indicate that exon 7 carries a cytoplasm targeting signal. When exon 7 was fused to a protein usually found in the nucleus, protein localization was largely shifted to the cytoplasm. Further testing revealed that the sequence QNQKE in exon 7 is responsible for this cytoplasmic redistribution (Zhang et al., 2003).

The SMN protein might have a distinct function among motor neurons, resulting in a tissue-specific manifestation of the disease. It was shown that SMN is part of another ribonucleoprotein (RNP) complex. Rossoll et al. suggest that a complex of SMN and heterogeneous nuclear ribonucleoprotein R (hnRNP-R) interacts with beta (ß)-actin. They have found that SMN-deficient motor neurons show reduced axon growth and reduced ß-actin levels (Monani, 2005; Rossoll et al., 2003). Other data links SMN to the Golgi apparatus and shows that SMN binds to α-coat protein complex (α-COP), which builds a complex with β-actin mRNA (Peter et al., 2011). Knockdown of α-COP by small interfering RNA (siRNA) led to the accumulation of SMN granules in the Golgi apparatus. When Golgi-mediated granule secretion is blocked, SMN levels in neurites were found to be decreased in NSC-34 cells. Knockdown of SMN in NSC-34 leads to reduced growth cone sizes. Additionally, when NSC-34 cells were treated with monesin, which leads to disruption of Golgi mediated granule secretion, smaller growth cone sizes were observed, similar to those observed in SMN knockdown experiments. These findings indicate that SMN granules may be transported through the Golgi apparatus (Ting et al., 2012).

There is also some evidence that SMN also plays a role in translational regulation. *In vitro* experiments showed that SMN dose-dependently represses the translation of a generic luciferase reporter. Further testing showed that the arginine methyltransferase co-activator associated arginine methyltransferase 1 (CARM1) is down-regulated when the SMN protein is present. This testing is in line with findings that CARM1 levels are higher in spinal cords of SMA mice and in fibroblasts from type SMA 1 patients (Sanchez et al., 2013).

SMA patients often develop osteopenia and therefore have increased fracture risk. SMA has been found to interact with osteoclast stimulatory factor and may contribute to the symptom of reduced bone density (Shanmugarajan et al., 2007). Other studies linked SMN to misregulation of glucose metabolism and pancreatic development. Bowerman et al. found aberrations in pancreatic islet composition, with a rise in glucagon-producing alpha cells and a decrease in insulin-producing beta cells. This leaves SMA carriers with the possibility of

developing metabolic disorders (Melissa Bowerman et al., 2014; Melissa Bowerman et al., 2012).

The SMN protein complex has several functions throughout the human body. From this point of view, it is understandable that loss of SMN leads to a variety in symptoms and severity.

1.1.5. Disease types

SMA is categorized into five categories. SMA type 0 manifests through either intrauterine death or respiratory distress at birth, which limits the life expectancy to three months. Type 0 children also show facial weakness and reduced fetal movement in the prenatal phase (Dubowitz, 1999; Macleod et al., 1999). SMA Type 1, described by Werdnig in 1894 and Hoffmann in 1900, is also called Werdnig-Hoffmann disease. The onset of type 1 disease occurs before the patients reach six months. The children never attain the ability to sit, display hypotonia and die due to respiratory distress, usually prior to reaching the age of two. In Type 2, onset usually occurs between 6–18 months. Affected patients are able to sit but cannot walk. Life expectancy is 10–40 years. With Type 3, also called Kugelberg-Welander disease, the patients can walk, and the onset occurs around the age of two years. Affected children attain the ability to walk independently, and their life expectancy is not limited. In Type 4, the onset occurs much later than in the other three forms of SMA, at about five years of age. Type 4 causes muscle weakness, but life expectancy is not reduced (Lefebvre et al., 1995; Barry S. Russman, 2007) (Table 1).

Type	Onset	Maximum Function Achieved	Life Expectancy
0	Prenatal	Needs respiratory support at birth	Fatal at birth without respiratory support
1	< 6 months	Sits with support only	< 2 years
2	6-18 months	Sits independentlly when placed	10-40 years
3	> 18 monts	Walks indenpendently ε 25 steps	Indefinte
4	> 5 years	Walks normally	Indefinte

Table 1: Disease types. Overview of the five types of SMA (taken from (Barry S. Russman, 2007).

A study published by Feldkötter et al. correlate the *SMN2* copy number and the type of SMA along with life expectancy. Patients with SMA Type 1 had better survival rates when they had two or three *SMN2* copies.

- Type 1: Children with one *SMN2* copy have risk of >99% developing Type 1 SMA. A child with two copies has risk of 97%. With three copies and four copies, the probabilities are as low as 7.2% and 1.6%.
- Type 2: A child with 3 copies of *SMN2* carries a 82.9% chance of developing Type 2 SMA, while patients with 4 copies of *SMN2*, have a 14.8% chance of developing Type 2 SMA. For 2 copies, the probability for Type 2 SMA is only 2.7%.
- Type 3: Children with 4 copies of *SMN2* have an 83.6% probability of developing Type 3 SMA. For 2 and 3 copies, the probabilities are 0.04% and 10% respectively (Feldkötter et al., 2002).

There are additional other correlations found to apply to SMA. Lefebvre et al. showed a correlation between SMN2 protein levels and disease severity (Lefebvre et al., 1997). Another correlation observed by Taylor et al. is between the age of onset and length of survival and *SMN2* copy number. A low copy number of *SMN2* was found to be associated with early onset and a lower survival rate (Taylor et al., 1998).

Another possible factor associated with disease severity is the neuronal apoptosis inhibitory protein (NAIP). The *NAIP* gene is localized on 5q13.2. Studies suggest that deletion of the *NAIP* gene also influences disease severity (Akutsu et al., 2002; Jedrzejowska et al., 2009; Roy et al., 1995). However, the role of *NAIP* in disease severity remains unclear. It is possible that loss of *NAIP* function occurs only due to its localization. The *NAIP* is localized in proximity to the *SMN1* gene, so it is therefore possible that the deletion affects both genes. Deletion of *NAIP* gene is associated with severe forms of SMA, which leads to the assumption that *NAIP* gene influences disease severity, but the validity of this claim remains unclear (Campbell et al., 1997).

1.1.6. Carrier screening

SMA is a recessive disease with a carrier frequency of 1:40–1:60 (Nurputra et al., 2013). Therefore, there are not only affected individuals, but also asymptomatic carriers, which can be screened (Verhaart et al., 2017). As gene testing would not suffice to determine whether a person is a carrier because those have a heterozygous deletion of *SMN1*, dosage testing is used to screen for SMA carriers. However, there are also limitations to dosage testing, since about 2% of SMA cases are due to *de novo* mutations in the *SMN1* gene and because the *SMN1* copy number in carriers can vary. About 4% of carriers carry three copies of *SMN1*. It

is also possible that a carrier has two copies on one chromosome and none on the other, which makes gene dosage testing unsuitable (Prior, 2008; Prior et al., 2010; Wirth et al., 1997). As such, there are two methods for carrier screening.

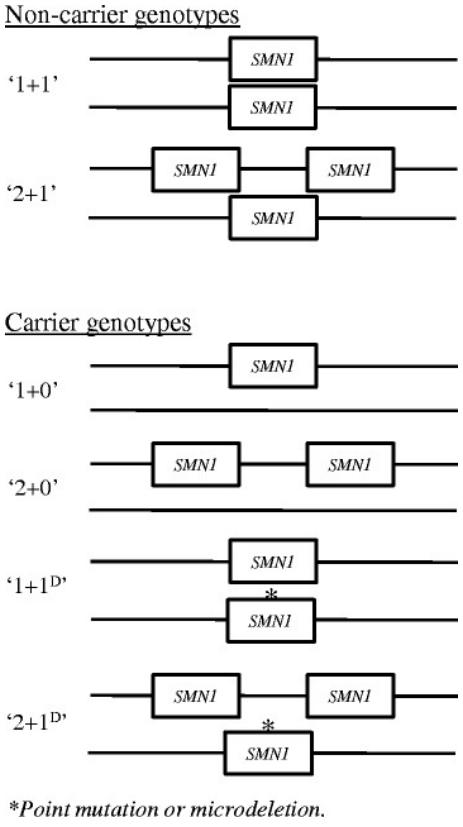

Figure 3: Spinal muscular atrophy genotypes. Some possible genotypes. (taken from (Verhaart et al., 2017)

One such method is a polymerase chain reaction (PCR) based analysis, PCR-Restriction fragment length polymorphism (RFLP) assay, or *SMN1* deletion assay. With the help of a mismatched reverse primer, a restriction site for DraI is cloned into the *SMN2* exon, but not in exon 7 of *SMN1*. The benefit of this method is that results can be obtained within 24 hours and that the outcome is unambiguous. However, this method does not screen for point mutations that lead to a loss of function in the *SMN1* gene (van der Steege et al., 1995). Another method is high-resolution melting analysis. This method is based on a nucleotide difference between *SMN1* and *SMN2* in exon 7. In intron 6 at position (−45) *SMN1* has a G while *SMN2* an A. An unlabeled probe that targets the G at intron 6 position −45 in *SMN1* is generated. The probe amplifies *SMN1* and *SMN2*, but for patients with only *SMN1*, that means, *SMN1* pairs perfectly with PCR probe, which leads to a higher melting temperature. The homozygous deletion of *SMN1* results in a lower melting temperature, producing three types of melting curves for the three genotypes: patients with *SMN1* deletion, patients with *SMN2* deletion, and healthy patients with *SMN1* and *SMN2*. The advantage of this method is

that mutations within the *SMN1* gene will decrease the DNA melting temperature (Chen et al., 2009). Morikawa et al. also presented melting curves that allow distinguishing between copy numbers of *SMN1* or *SMN2* (Morikawa et al., 2011). Carrier screening is an important method to define carrier status of a person, but there are drawbacks to carrier screening,

It remains controversial whether universal carrier screening should be available for women or couples who either are planning on having a child or are already expecting a child. There are many factors, such as the cost for screening that should be taken under consideration. It is also not possible to predict disease severity of a possibly affected child and one has to keep in mind that there may be new treatment options for SMA in the future, which could increase quality of life and life expectancy (Little et al., 2010).

Newborn screening, on the other hand, can be very useful to enable affected children to enter clinical trials as soon as possible. The other advantage is the possibility of an early treatment. Affected newborns could also be tested for *SMN2* copy number, in order to obtain a prognosis on disease severity (Prior et al., 2010).

In order to address this controversial issue the World Health Organization (WHO) established some guidelines, more than 50 years ago that should help to address this issue. The WHO recommends ten criteria for screening programs, namely the Wilson-Jungner criteria, published in 1968. Although these are still valuable, many adaptations of the Wilson-Jungner criteria can be found, due to the scientific progress of the past 50 years. SMA does not meet the second of the ten criteria, which states that "there should be an accepted treatment for patients with recognized disease"(Wilson et al., 1968). Another factor that should be taken under consideration when discussing carrier screening is the effect of a false positive test. A false positive test can bring distress and anxiety upon parents and influence their reproductive decisions (Andermann et al., 2008; Orzalesi & Danhaive, 2009; Wilson et al., 1968).

1.1.7. Therapeutic possibilities

There is no cure for SMA. However, different therapeutic possibilities are still under investigation. These therapeutic approaches can be divided into three groups.

1.1.7.1. Non-SMN targets

One therapeutic approach to treat SMA is to protect patients from motor neuron loss. Amyotrophic lateral sclerosis (ALS) is neurodegenerative disease that also manifests in loss of motor neurons. This disorder has been linked to glutamate-induced excitotoxicity.

Glutamatergic neurotransmission in ALS patients is impaired, which leads to loss of motor neurons (Heath & Shaw, 2002). Riluzole, an anti-excitotoxic agent, has been tested and used for ALS therapy (Louvel et al., 1997). It is possible that SMA patients could also profit from riluzole treatment. In a Phase I trial, Russman et al. tested the effects of riluzole on SMA patients. They found a positive effect in the treatment with riluzole and no negative side effects were observed. However, this study was based on a small sample and short duration (B. S. Russman et al., 2003).

β–lactam antibiotics are another drug with potential neuroprotective functions. Treatment of ALS-mice with ceftriaxone, a β–lactam antibiotic, for a period of two weeks led to delay in motor neuron loss. Glutamate transporters are known to prevent glutamate neurotoxicity. Rothstein et al. suggest that this arises from an increase of glutamate transporter 1 (GLT1) expression upon ß-lactam treatment (Rothstein et al., 2005). Nizzardo et al. tested the effect of ceftriaxone, a β-lactam antibiotic, on SMA mice. The treated mice showed a slightly prolonged lifespan and an increase in bodyweight. Ceftriaxone has a neuroprotective effect in SMA as well. This effect is achieved through the increased expression of the glutamate transporter GLT1, an increase in the transcription factor NRF2 and in SMN protein (Nizzardo et al., 2011).

Olesoxime (TRO19622) has been found to act as a neuroprotective agent in ALS. *In vivo* studies showed that not only does TRO19622 possesses neuroprotective ability, but also a neuroregenerative one. Olesoxime has been found to interact with translocator proteins (TSPOs) and voltage-dependent anion channels (VDACs), which are both components of the mitochondrial permeability pore. Studies on SMA patients are ongoing (Bordet et al., 2007). A Phase-II study has found that olesoxime treatment may be beneficial for SMA patients (Dessaud et al., 2014).

There are other factors that are not directly related to the nervous system but may also be taken under consideration as targets of investigation for therapy. Bowerman et al. have shown that SMN depletion alters the RhoA/ROCK pathway. Mice treated with a ROCK inhibitor showed a positive effect on NMJ maturation and muscle fiber size, as well as prolonged lifespan (Mélissa Bowerman et al., 2010). Another study observed that maternal diet can influence the lifespan of an $SMN^{\Delta 7}$ mouse model. Animals that were fed a diet higher in fat had a prolonged lifespan compared to animals on a lower fat diet (Butchbach et al., 2010). Muscle training may also be beneficial for SMA patients. A study performed on SMA Type 3 and Type 3 patients showed that resistance strength training led to improvement in motor

function (Lewelt et al., 2015). Cunha et al. showed that physical therapy in combination with hydrotherapy has a beneficial effect on SMA type 2 and 3 patients (Cunha et al., 1996).
Another possible approach to treat SMA is stem cell therapy. Corti et al. have shown that stem cell transplantation of neuronal stem cells leads to extended lifespan and has a positive effect on weight and motor neuron number (Corti et al., 2008).

1.1.7.2. Targeting SMN2

Alternative splicing results in only about 10% of SMN2 protein being full-length SMN protein that still includes exon 7 (Jodelka et al., 2010). This phenomenon opens up a possible approach to target SMN2 for therapeutic measures. In a drug screening process for SMA, one compound that stood out was sodium butyrate. Lymphoid cells from SMA patients treated with sodium butyrate showed a higher amount of full-length SMN. *In vivo* studies on mice also showed an increase in full-length SMN protein amounts in different cell types, including the motor neurons of the spinal cord. The mice also showed an increased lifespan. Sodium butyrate acts most probably through *SMN* splicing (Chang et al., 2001). Sodium butyrate is a histone deacetylase (HDAC) inhibitor (Boffa et al., 1978). There are studies on other HDAC inhibitors. Valproic acid (VPA) treated fibroblast from SMA patients showed an increase in full-length SMA protein levels in a dose-dependent manner. VPA increases SMN protein levels by up-regulation of SMN2 via stimulation of exon 7 inclusion. Htra2-β1 was shown to increase the inclusion of exon 7, leading to an increase in full-length protein. Treatment with VPA leads to an increased level of Htra2-β1; however, not only Htra2-β1, but also the two splicing factors SF2/ASF and SRp20 were found to be up-regulated upon VPA treatment. Treatment with butyrate produced the same effect, which leads to the assumption that butyrate and VPA act similarly (Brichta et al., 2003; Hofmann et al., 2000).
There are also non-HDAC inhibitor drugs that promote inclusion of exon 7. When patient lymphoblastoid cells were treated with hydroxyurea, a rise in full-length protein levels was observed, whereas total SMN mRNA amounts remained stable. This result indicates that hydroxyurea does not act on the transcriptional level, but promotes the inclusion of exon 7 (Grzeschik et al., 2005). $SMN^{\Delta 7}$ is less stable than the full-length SMN protein (C. L. Lorson et al., 1999; Christian L. Lorson et al., 1998). Increasing $SMN^{\Delta 7}$ stability may be a possible target for therapy. Aminoglycosides antibiotics act on prokaryotic ribosomes, but they are also known to interfere with eukaryotic translational machinery. Aminoglycosides can lead to a read-through of stop codons. In the case of an SMN protein, aminoglycosides promote a

read-through of the initial stop codon in exon 8, which leads to a longer C-terminal sequence, resulting in higher protein-stability. When SMA patient fibroblast cells were treated with amikacin or tobramycin, two aminoglycosides, increased SMN levels were found (Wolstencroft et al., 2005).

In 2017, Biogen brought Spinraza® (nusinersen) onto the market. Nusinersen is the first medication for SMA to be approved by the United States Food and Drug Administration (FDA) (Corey, 2017). The FDA states in their 2016 press release:

> The U.S. Food and Drug Administration today approved Spinraza® (nusinersen), the first drug approved to treat children and adults with spinal muscular atrophy (SMA), a rare and often fatal genetic disease affecting muscle strength and movement. Spinraza® is an injection administered into the fluid surrounding the spinal cord.

Spinraza® is an antisense oligonucleotide (ASO) that inhibits splicing factor binding to pre-mRNA by blocking the recognition site; thereby promoting the inclusion of exon 7 (Corey, 2017).

1.1.7.3. SMN1 replacement

Another therapeutic possibility is the delivery of SMN protein. Azzouz et al. were the first group to successfully deliver SMN protein via a lentivirus. They first tested lentivector-mediated SMN replacement in fibroblasts of SMA Type 1 patients. They observed a twofold increase in gem numbers. In the next step, they tested SMN replacement in SMN mice. The SMN-treated mice showed a delay in weight loss, a 3–5 day lifespan increase and improved motor neuron survival (Azzouz et al., 2004). In another study, SMA mice were treated with self-complementary adeno-associated virus (scAAV) 9-SMN at different postnatal points in time. Postnatal day 2 (P2)-treated mice showed the highest increase in lifespan and body mass. The effect on P5-treated mice has decreased, and P10-treated mice showed almost no effect. This indicates that there is a critical time in motor neuronal development in which treatment is most beneficial. Furthermore, the scAAV9's ability to cross the blood-brain-barrier (BBB) was tested. A P1 male cynomolgus macaque was injected with scAAV9-GFP. A green fluorescent protein (GFP) signal was found in motor neurons (Foust et al., 2010). The self-complementary AAV vector (scAAV) has a double-stranded deoxyribonucleic acid (DNA) genome. ScAAV gene expression has an earlier onset than that of single-stranded AAV. Treatment with scAAV SMN led to an increase of 157 days in median survival (Passini

et al., 2010). ScAAVs can initiate expression sooner, depending on the tissue in which they are expressed (McCarty, 2008).

Dominguez et al. produced a scAAV9 vector with a codon optimized *SMN1* sequence. Codon optimization is used to achieve higher protein levels. Furthermore, a chimeric intron was placed downstream of the strong phosphoglycerate kinase (PGK) promoter to overexpress *SMN* in a severe SMA mouse model. An increase of life expectancy from 27 to over 340 days was observed as a result. The mice from the control group usually survive about 13 days. They showed a substantial improvement in body weight compared to non-treated mice and are rescued from motor neuron death. The animals were treated as of postnatal day 1 (Dominguez et al., 2011) .

A 2018 study raises some safety concerns regarding high-dose intravenous administration of adeno-associated virus-vector-expressing human *SMN*. A toxic effect in nonhuman primates (NHPs) and piglets was observed (Hinderer et al., 2018).

1.2. Trans-activating transcriptional activator proteins

Another possible strategy is to deliver proteins directly into the cell. However, in this process the SMN has to be fused to a sequence that would enable it to cross the BBB. Trans-activating transcriptional activator (TAT) proteins were found to be taken up by the cell and to cross the BBB (Cao et al., 2002; Frankel & Pabo, 1988; Green & Loewenstein, 1988).

The human immunodeficiency virus (HIV) encodes for several proteins. In addition to the structural proteins gag, pol and env. HIV Type 1 also encodes to regulatory proteins. One of these proteins is the TAT protein. The HIV-TAT regulates viral gene expression by binding to the transactivation response element (TAR) in the long terminal repeat (LTR) sequence of HIV-1. Depending on the viral subtype, the length of HIV-TAT varies from 86 to106 amino acids. The HIV-TAT is encoded by 2 exons (Zou et al., 2017).

In 1988, Green and Pabo (Frankel et al., 1988; Green et al., 1988) independently discovered that HIV-TAT crosses cell membranes and can transactivate the viral genome (Becker-Hapak et al., 2001). Not all 86 amino acids residues are essential for cellular uptake. Deletion studies have shown that the basic domain of TAT, termed the protein transduction domain (PTD) is sufficient for cellular uptake. TAT-fusion constructs that contained the complete TAT-PTD were taken up by the cell and accumulated in the nucleus (Vivès et al., 1997).

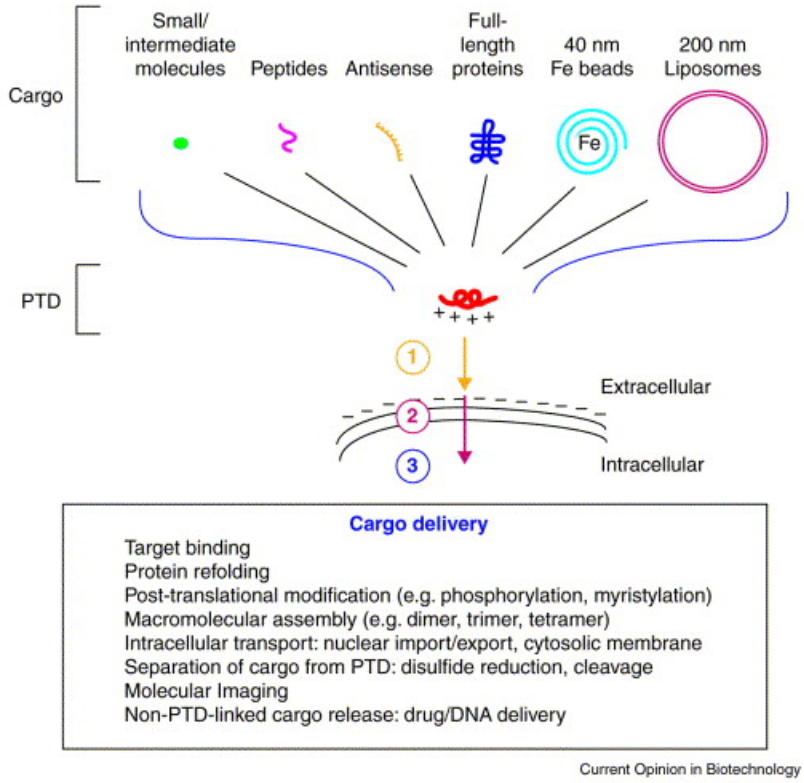

Figure 4: The arginine-dependent protein transduction domains (PTDs). Various cargos can be transported via the PTD (taken from (Wadia & Dowdy, 2002).

The TAT protein was delivered *in vivo* into mice. Schwarze et al. examined a 120 kDa β-galactosidase protein injected into mice and delivered into the liver, heart muscle, kidney and spleen. β-galactosidase TAT fusion protein was successfully delivered into the brains of mice (Schwarze et al., 1999). Urea-denaturated fusion proteins seem to transduce more efficiently into the cells than their non-denaturated counterparts (Nagahara et al., 1998). Furthermore, denatured TAT-p27^{WT} was able to induce cell migration, when added to cells. In contrast, correctly folded TAT-p27^{WT} was not able induce cell migration (Nagahara et al., 1998). If TAT proteins can cross the BBB, then they also can be used to deliver protein into CNS cells. A Bcl-xL fusion protein was shown to inhibit staurosporin (STS)-induced apoptosis in cultured neurons. The inhibition was similar in previously treated cells to post-treated cells. *In vivo* experiments showed preischemic treatment of mice with Bcl-xL fusion protein reduced infarct volume (Cao et al., 2002).

There are some limitations regarding TAT-mediated protein delivery that should be considered. Every fusion protein will have a different half-life, and there are also proteins that have a tight conformation at the *N*-terminus, so that the TAT domain might be covered or buried (Becker-Hapak et al., 2001). The mechanism by which TAT proteins are taken up by the cell remains unclear. TAT translocation seems to be temperature independent. Studies have shown that TAT is still translocated at 4°C (Vivès et al., 1997). Uptake via endocytosis

is blocked at 4°C (Weigel & Oka, 1981). Other studies have shown that TAT is translocated in an adenosintriphosphate (ATP) independent way. Cells treated with sodium azide or rotenone, which have an ATP inhibitory effect, showed no inhibition of TAT uptake (Suzuki et al., 2002). However, recent studies paint a different picture. Richard et al. have shown that TAT protein uptake has been inhibited at 4°C, that ATP inhibition also led to the abrogation of cellular uptake of TAT protein, and that endocytosis might be a mode of cellular uptake (Richard et al., 2005; Richard et al., 2003). One of the main advantages of TAT protein-mediated delivery is that TAT seems not have a toxic effect on the cells in which it is delivered. Concentrations of 5 mg/mL of TAT showed no cytotoxic effect (Baoum et al., 2012). Suzuki et al. found no cytotoxicity of 100 μM TAT (48-60) on HeLA cells, after 24 hour incubation time (Suzuki et al., 2002).

1.3. Aim of this thesis

In SMA, a loss or a deficiency of full-length SMN protein leads to motor neuron loss and muscle weakness. Presently there is no efficient treatment for this disease. Studies have shown that SMN delivery to affected cells can lead to improvement in motor neuron function, bodyweight and lifespan (Azzouz et al., 2004). The first part of the study focuses on establishing a proper protocol for the purification of TAT-SMN1 from bacterial lysates. Next, the thesis focuses on the purified TAT-SMN1 protein. We tested the protein's ability to enter cells. Further we analyzed the protein's stability and its cytotoxicity. The last part of the thesis deals with the generation of a bacterial expression plasmid containing *SMN1* without the TAT sequence.

2. Materials

2.1. Chemicals	Product Number	Supplier
2-Mercaptoethanol	M3148-25M	Sigma-Aldrich®
2-Propanol	278475	Sigma-Aldrich®
LB-Agar (Miller)	1.10283.0500	Merck
Ammonium persulfate (APS)	A3678	Merck
Benzonase® nuclease	E1014-25KU	Sigma-Aldrich®
Bio-Rad protein Assay Dye Reagent Concentrate	500-0006	Bio-Rad Laboratories
Bovine serum albumin (BSA)	A9647	Sigma-Aldrich®
Bromphenol blue	B0126	Sigma-Aldrich®
Calcium chloride	10043-52-4	Carl Roth®
Brilliant Blue R, 250	27816-54	Sigma-Aldrich®
4′,6-Diamidin-2-phenylindol (DAPI)	32670	Sigma-Aldrich®
Dimethyl sulfoxide (DMSO)	D2650	Sigma-Aldrich®
Ethylenediaminetetraacetic acid (EDTA)	EDS	Sigma-Aldrich®
Egtazic acid (EGTA)	3054.1	Carl Roth®
Fixmilch Instant (sofortlösliches Magermilchpulver)	115710-10	MaresiAustria GmbH®
Fluoprep	75521	bioMérieux
Midori Green Direct	617006	Biozym®
Gentamycin solution	G1397	Sigma-Aldrich®
Glycerol	G2025	Sigma-Aldrich®
Glycine	S0046	Sigma-Aldrich®
Imidazole	12399-1004	Sigma-Aldrich®
Isopropyl-β-D-thiogalactoside (IPTG)	1675814	Sigma-Aldrich®
Kanamycin sulfate	10106801001	Sigma-Aldrich®
Lysozyme from chicken egg white	L379010X1ML	Sigma-Aldrich®
Meat extract for microbiology	70164	Fluka™

Chemicals	Product Number	Supplier
Methanol	19091	Carl Roth®
Sodium azide	S2002	Sigma-Aldrich®
Nonidet-P40	11754599001	Sigma-Aldrich®
PageRuler™ Prestained Protein Ladder	26616	Thermo Fisher Scientific
Paraformaldehyde	158127	Sigma-Aldrich®
Penicillin-Streptomycin	15140122	Gibco® by Life Technologies™
Phenylmethanesulfonyl fluoride (PMSF)	93482	Sigma-Aldrich®
Ponceau-S	1142750010	Merck
Potassium chloride (KCI)	1049361000	Merck
Potassium phosphate monobasic (KH2PO41	1048771000	Merck
Protease Inhibitor Cocktail (l00X)	8340	Sigma-Aldrich®
S.O.C. Medium	15544034	Thermo Fisher Scientific
Sodium chloride (NaCI)	S3014	Sigma-Aldrich®
Sodium deoxycholate	D6750	Sigma-Aldrich®
Sodium dodecyl sulfate (SDS)	428023	Merck
Sodium fluoride (NaF)	S7920	Sigma-Aldrich®
Sodium orthovanadate	S6508	Sigma-Aldrich®
Sodium phosphate dibasic dihydrate	1065801000	Merck
N,N,N',N'-Tetramethyl ethylenediamine (TEMED)	1107320100	Merck
Triton X-100	T-8787	Sigma-Aldrich®
Trizma® base	T6066	Sigma-Aldrich®
Tryptone/Peptone ex casein	8952.3	Carl Roth®
Tween® 20	P9416	Sigma-Aldrich®
Urea	57-13-6	Merck
X-Gal Solution	R0941	Thermo Fisher Scientific
Yeast Extract Technical	288620	BD Biosciences

Table 2: Chemicals and suppliers

2.2. Kits	Product Number	Supplier
ChemiGlow™ West Chemiluminescence Substrat Kit (Stable Peroxide Butter and Luminol/Enhacer Solution)	60-12597-00	ProteinSimple®
EZ4U Kit	BI-5000	Biomedica
GenElute™ Plasmid Miniprep Kit	PLN10	Sigma-Aldrich®
Micro BCA™ protein Assay Kit	23235	Thermo Fisher Scientific
QIAquick® Gel Extraction Kit	28704	Qiagen

Table 3: Kits and suppliers

2.3. Antibodies	Product Number	Supplier
His-Tag Polyclonal Antibody	2365	Cell Signaling Technology
6-His Affinity Purified Antibody	18814	QED Bioscience Inc.
anti-6X His tag® antibody	ab9108	Abcam
anti-alpha Tubulin antibody - Loading Control	ab4074	Abcam
anti-Gemin 3 antibody [EPR11283]	ab11283	Abcam
anti-Mouse lgG	A4416	Sigma-Aldrich®
anti-Rabbit lgG	A0545	Sigma-Aldrich®
Goat anti-Mouse IgG H&L (Alexa Fluor® 488)	ab150113	Abcam
Goat anti-Rabbit IgG H&L (Alexa Fluor® 568)	ab175471	Abcam
His Tag antibody	orb66653	Biorbyt
Monoclonal antibody to HIV-1 TAT basic domain	A07H02010A-031	ACRIS
Monoclonal anti-SMN antibody produced in mouse	S2944	Sigma-Aldrich®
STREB MAB Classic conjugated to horseradish peroxidase	1509-007	IBA

Table 4: Antibodies and suppliers

2.4. Restriction Enzymes, Ligases, dNTPs and Buffers	Product Number	Supplier
dNTP Mix	18427013	Invitrogen™
Bovine Serum Albumin (100X)	B9001	New England Biolabs® Inc.
BsrGI	R0575S	New England Biolabs® Inc.
BsrGI-HF®	R3575S	New England Biolabs® Inc..
CutSmart® Buffer	B7204S	New England Biolabs® Inc.
EagI-HF®	R3505S	New England Biolabs® Inc.
EcoRV	R0195S	New England Biolabs® Inc.
ExoSAP-IT™ PCR Product Cleanup Reagent	78200.200.UL	Thermo Fisher Scientific
GoTaq® Green Master Mix	M7121	Promega
NcoI	R0193S	New England Biolabs® Inc.
NcoI-HF®	R3193S	New England Biolabs® Inc.
NdeI	R0111S	New England Biolabs® Inc.
NEBuffer™ 1	B7001S	New England Biolabs® Inc..
NEBuffer™ 3	B7203S	New England Biolabs® Inc.
Pfu DNA Polymerase	M7741	Promega
SacI-HF®	R3156S	New England Biolabs® Inc.
SalI-HF®	R3138S	New England Biolabs® Inc.
T4 DNA Ligase Reaction Buffer	B0202S	New England Biolabs® Inc.

Restriction Enzymes, Ligases, dNTPs and Buffers	Product Number	Supplier
T4 RNA Ligase 1	N0204S	New England Biolabs® Inc.

Table 5: Restriction Enzymes, Ligases, dNTPs and Buffers

2.5. Columns and Buffers	Product Number	Supplier
EndoTrap ® blue - Endotoxin Removal	311064	Hyglos GmbH
EndoTrap® HD 5X Regeneration Buffer	311067	Hyglos GmbH
His Gravi Trap	11-0033-99	GE Healthcare
PD10	17-0851-01	GE Healthcare

Table 6: Columns, buffers and suppliers

2.6. Ruler/Loading dye	Product Number	Supplier
GeneRuler 1 kb Plus DNA Ladder	SM1334	Thermo Fisher Scientific
PageRuler™ Prestained protein Ladder	26616	Thermo Fisher Scientific
DNA Gel Loading Dye (6X)	R0611	Thermo Fisher Scientific

Table 7: Ruler, loading dye and suppliers

2.7. Cell culture material	Product Number	Supplier
DMEM (lX)	41695-039	Gibco® by Life Technologies™
DMEM (lX)	41966-029	Gibco® by Life Technologies™
Fetal Bovine Serum	F9665	Sigma-Aldrich®
Fetal Bovine Serum	F4135	Sigma-Aldrich®
0.25% Trypsin-EDTA 1X	25200-056	Gibco® by Life Technologies™

Table 8: Cell culture material and suppliers

2.8. Instruments	Product Number	Supplier
Branson Sonifier™ 450	1145035-16	Branson
ChemiDoc™ Touch Gel Imaging System	1708370	Bio-Rad Laboratories Inc.
FluorChem HD2 system	92-15098-0	Protein Simple
Fully Automated Inverted Research Microscope for Biomedical Research Leica DMI6000 B	DMI6000 B	Leica Biosystems
Microplate Rectder, Perkin Eimer Wallac 1420 Victor2 Multilabel Counter	PE-WV22	Marshall Scientific LLC®
Mupid-One	613000	Biozym®
PowerPac™ HC High-Current Power Supply	1645052	Bio-Rad Laboratories

Table 9: Measuring instruments, imaging instruments and suppliers

2.9. Other laboratory material	Product Number	Supplier
Cellstar® cell culture flask, 50 ml, 25 cm²	690 170	Greiner Bio-One®
Cellstar® cell culture flasks, 250 ml, 75 cm^2	658 170	Greiner Bio-One®
Falcon™ Chambered Cell Culture Slides	08-774-25	Thermo Fisher Scientific
Microplate 96-well	655161	Greiner Bio-One®
Nitrocellulose Membranes 0.2 µm	162-0112	Bio-Rad Laboratories
Amicon Ultra-4, PLGC Ultracel-PL Membran, 10 kDa	UFC801024	Merck

Table 10: Other laboratory material and suppliers

2.10. Primers	Sequence
pET28_R1	CGCAGCGTGACCGCTACACTTG
peT28F1seq	CGATGCGTCCGGCGTAGAGGATCG
Primer T7	TAATACGACTCACTATAGGG

Primers	Sequence
NcoI_His	CCCCCCCCATGGCATATGGACACCACCATC ACCACCATCCCACCGCGATGAGCAGCGGCG
BsrGI_Strep	CCCCCCTGTACAGACCACCGTTCAGGCT

Table 11: Primers

2.11. Plasmids	Supplier
pBluescript	Laccone Lab
pET28_HisTAT_SMN1_Strep	Laccone Lab
pJexpress411:64109 - TAT_SMN1_Strep_MOD	Laccone Lab

Table 12: Plasmids

2.12. Buffers and Working solutions	
Blocking solution (1% BSA in PBS)	
BSA	1%
in 1X PBS	
Blocking solution (StrepMAB-Classic conjugated to horseradish peroxidase):	
BSA	3%
Tween	0.5%
in 1X PBS	
Blocking solution (5% milkpowder)	
Milk powder	5%
Tween	0.1%
in 1X TBS	
Complete lysis buffer ready to use	
Lysis buffer w/o inhibitors	960 µl
0.5 M NaF	10 µl
0.1 M Na-orthovanadate	10 µl
0.1 M PMSF	10 µl
Protease Inhibitor Cocktail 100X	10 µl

Coomassie blue staining solution	
Coomassie R250	1 g
Acetic acid	100 ml
Methanol	400 ml
ddH_2O	500 ml
DAPI 1:1000 in PBS	
DAPI	0.02 g
Dissolve in 20 ml PBS	
Destaining solution	
Acetic acid	100 ml
Methanol	200 ml
ddH_2O	700 ml
HIS Gravi Trap Binding buffer (pH=8)	
Urea	8 M
Tris-HCl	20 mM
NaCl	500 mM
Glycerol	10%
Imidazole	20 mM
(ß-mercaptoethanol)	1 mM
HIS Gravi Trap Elution buffer (pH=8)	
Urea	8 M
Tris-HCl	20 mM
NaCl	500 mM
Glycerol	10%
Imidazole	500 mM
(ß-mercaptoethanol)	1 mM
LB agar	
Agar	7.4 g
ddH_2O	200 ml
Autoclave	

LB medium	
Bacto-tryptone	1%
Yeast extracts	0.5%
NaCl	1%
Adjust pH to 7.2 and autoclave.	
LB (rich) medium	
Bacto-tryptone	1%
Yeast extracts	0.5%
NaCl	1%
Meat extract	0.25%
Adjust pH to 7.2 and autoclave.	
Lysis buffer (Protein purification)	
Urea	8 M
Tris-HCl	20 mM
NaCl	500 mM
Glycerol	10%
Imidazole	20 mM
ß-mercaptoethanol	1 mM
Lysozyme	0.2 mg/ml
Benzonase®Nuclease	10 U/ml
Phenylmethylsulfonyl fluoride (PMSF)	1 mM
Protease inhibitor for HIS-tagged proteins	1x
Lysis buffer (1X stock) without inhibitors	
10X TBS, pH=7.4	1 ml
10% Triton X-100	1 ml
0.5M EDTA	20 µl
0.25M EGTA	40 µl
1% SDS	500 µl
5% Na-deoxycholate	200 µl
10% Nonidet-P40	2 ml

ddH_2O	4.8 ml
Store at 4°C	
Formaldehyde fix solution 4% (w/v)	
Paraformaldehyde	4 g
PBS	100 ml
Heat and stir	
Adjust pH to 7.2	
Store at -20°C	
PD-10 Elution buffer 1 (pH=7)	
Tris-HCl	20 mM
NaCl	200 mM
Glycerol	10%
PD-10 Elution buffer 2 (pH=7)	
Tris-HCl	20 mM
EDTA	0.1 mM
Glycerol	10%
6X SDS sample buffer	
Glycerol	6 ml
Tris-HCl	7 ml
Bromphenol blue	0.0024 g
SDS	2 g
Fill up to 20 ml with ddH_2O.	
Store at -20°C.	
β-mercaptoethanol (add to samples before denaturing them at 95°C.)	5%
10X PBS	
ddH_2O	800 ml
KCl	2 g
Na_2HPO_4	14.4 g
KH_2PO_4	2.4 g
Adjust pH to 7.4	

Adjust volume to 1 L with ddH_2O	
Autoclave	
12% SDS-PAGE gel ingredients	
Separation gel (12%)	
ddH_2O	4.9 ml
ProSieve™ 50 Gel Solution	2.4 ml
1.5 M Tris-HCl pH=8.8	2.5 ml
10% SDS Solution	100 µl
10% APS	100 µl
TEMED	4 µl
Stacking Gel (5%)	
ddH_2O	3.75 ml
ProSieve™ 50 Gel Solution	0.5 ml
1M Tris-HCl pH=5.8	0.65 ml
10% SDS Solution	50 µl
10% APS	50 µl
TEMED	5 µl
10X SDS running buffer	
Tris	30 g
Glycine	144 g
SDS	10 g
Dissolved in 1 L ddH2O	
10X TBS	
ddH_2O	900 ml
Tris base	24 g
NaCl	88 g
Adjust pH to 7.6.	
Adjust volume to 1 L with ddH_2O.	
Autoclave	
Tris base	121.1 g

Boric acid	61.8 g
EDTA	7.4 g
dissolved in 1 L ddH_2O	
10X TBE Buffer	
Tris base	121.1 g
Boric acid	61.8 g
EDTA	7.4 g
dissolved in 1 L ddH_2O	

Table 13: Buffers and working solutions

3. Methods

TAT fusion proteins can be expressed in bacteria from vectors containing an 11 bp transduction domain. Protein can be isolated from bacterial pellets by sonication under denaturing conditions with the lysis buffer containing 8 M urea (Becker-Hapak et al., 2001).

3.1. DNA Methods

3.1.1. Agarose gels

One percent agarose gels were prepared by dissolving agarose in 1X TBE buffer. Midori Green was added after the gel cooled down to lukewarm temperature. The 6X loading dye was added to the samples before they were loaded on the gel. The gels were run for 25–35 minutes at 135 volts (V).

3.1.2. PCR reactions and programs

PCR reaction mix 1

Pfu DNA Polymerase Puffer 10X	2 µl
dNTP MIX, 10 µM each	0µl
Primer NcoI_His (10 µM)	1 µl
BsrGI_Strep (10 µM)	1µl
Pfu DNA Polymerase (3 U/µl)	0.2 µl
DNA template	0.2 µl
H_2O	1.5 µl
Total volume	20 µl

PCR cycling program 1:

95°C	2 minutes	
95°C	30 seconds	36 cycles
65°C	30 seconds	
73°C	2 minutes	
73°C	5 minutes	
4°C	∞	

PCR reaction mix 2

H_2O	7 µl
Primer pET28 F1seq	1 µl
Primer pET28 R1 seq	1 µl
Green MM	10 µl
Ligation/Insert/Vector/H_2O	1 µl
Total volume	20 µl

PCR cycling program 2

95°C	3 minutes	
95°C	30 seconds	36 cycles
63°C	30 seconds	
72°C	1 minutes 20 seconds	
72°C	3 minutes	
4°C	∞	

3.1.3. Restriction digest reactions

Restriction digest of pBluescript SK with EcoR

NEBufffer 3 (10X)	2 µl
BSA (100X)	0.2 µl
EcoRV	0.2 µl
Nuclease free H_2O	14.6 µl
pBluescript (midiprep 12.03.1993)	3 µl
Total volume	20 µl
for 3 hours at 37°C	

Control digest mix

CutSmart 10X Buffer	2 µl
NcoI-HF/SaII-HF/NdeI	0.2 µl
BsrGI-HF/Eag-HF/SacI-HF	0.2 µl
H_2O	12.6 µl
sample	5 µl
Total volume	20 µl

for 2 hours at 37°C

NcoI and BsrG1 restriction digest

sample 2,3,4,5	12 µl
Cut Smart 10X Buffer	2 µl
NcoI	2.6 µl
BsrG1	2.6 µl
H_2O	0.8 µl
Total volume	20 µl

for 2 hours at 37°C

NcoI and BsrG1 restriction digest

pET28	3 µl
Cut Smart 10X Buffer	2 µl
NcoI	0.2 µl
BsrGI	0.2 µl
H_2O	14.6 µl
Total volume	20 µl

for 2 hours at 37°C

3.1.4. Ligation

Ligation mix 1

Vector DNA	5 µl
Insert DNA	9 µl
T4 DNA ligase	1 µl
T4 DNA ligase puffer	2 µl
H_2O	3 µl
Total volume	20 µl

+ 0.1 µl EcoRV was added and the ligation was incubated for 2 hours at room temperature, afterwards 0.1 µl EcoRV was added and the ligation was incubated for 30 minutes at 37°C. In the last step the ligation was incubated for 10 minutes at 65°C.

Ligation mix 2

Vector DNA	5 µl
Insert DNA	12 µ
T4 DNA Ligase	1 µl
T4 DNA Ligase 10X Puffer	2 µl
Total volume	20 µl

Incubate for 2 hours at 37°C and for 10 minutes at 65°C.

3.1.5. DNA extraction from gel

The DNA was extracted from gel using QIAquick® Gel Extraction Kit (Qiagen) according to the manufacturer's instructions.

3.1.6. Overnight cultures

Five transformants were picked, and overnight cultures were grown in a medium containing gentamycin and kanamycin for the selection of the expressed plasmid at 37°C. One colony

was picked from the plate and inoculated in 10 mL LB-kanamycin/gentamycin medium overnight at 37°C and 220 rpm

3.1.7. Minipreparation

A 50 µl vial of One-Shot Top 10 competent cells was thawed on ice, 5 µl of the ligation was added to the cells, and the cells were incubated on ice for 30 minutes. The bacteria cells were heat-shocked for 30 seconds at 42°C. After heat-shock, the bacteria were incubated on ice. Then, 250 µl pre-warmed (42°C) SOC media was added, after which the bacteria were incubated for 1 hour at 37°C and 220 rpm and then plated on LB-plates and incubated overnight at 37°C. The ligation was plated on X-Gal LB-ampicillin plates and incubated overnight at 37°C. Twelve colonies were put in tubes with 3 ml LB-ampicillin medium (1 colony each) and incubated overnight at 37°C and 220 rpm. 1.5 ml of the culture medium was used for DNA extraction. The DNA was extracted using GenElute™ Plasmid Miniprep Kit (Sigma) according to the manufacturer's instructions.

3.1.8. Construct map

The *TAT-SMN1* gene is cloned into pET28 vector, which has a kanamycin resistance. The TAT-SMN1 protein has HIS-Tag and a Strep-TAG.

Figure 5: pET28_HisTAT_SMN1_Strep. Construct of TAT-SMN1 in pET28 Vector.

3.1.9. Transformation

Arctic Express (DE3) *E. Coli* cells were transformed with the protein expression plasmid using a 37°C cultivation temperature. Arctic Express cells were thawed on ice. A 2 µl XL10-Gold β-mercaptoethanol mix was added to the cells, 0.5 ml of plasmid DNA was added, and the cells were incubated on ice. The bacteria cells were heat shocked for 20 seconds at 42°C. 900 µl prewarmed (42°C) S.O.C. medium was added. The bacteria were then incubated for 1 hour at 37°C and 220 rpm and then plated on LB-plates and incubated overnight at 37°C.

3.2. Protein Methods

3.2.1. Isopropyl-*β*-D-thiogalactopyranosid (IPTG) induced protein production

The cells were grown without antibiotic selection for 5 hours at 30°C and 220 rpm. The culture medium was then incubated for 1 hour on ice and diluted 1:10 in LB-rich medium and incubated for 15 minutes at 12°C. Protein expression was induced with IPTG overnight at 12°C in the dark. Cells were centrifuged for 20 minutes at 4.000 xg and 4°C. Pellets were stored at -80°C.

3.2.2. Cell lysis

E. coli pellets were thawed on ice for 15 minutes. The pellets were pooled and lysed in 20 ml bacterial lysis buffer (8 M urea) per 1 g pellet. The lysate was incubated for 30 minutes at room temperature and ultra-sonicated (6X 1 minute with 2 minute cooling period). After ultra-sonication the lysate was centrifuged at 18.000 xg at room temperature. The supernatant was filtered in a new tube with a 0.45 µm filter.

3.2.3. Histrap affinity chromatography

The HIS-tagged TAT-SMN1 protein was purified using a HIS Gravi Trap Column (GE Healthcare). The column was washed with 5 ml elution buffer and with 10 ml binding buffer. Then the column was equilibrated with binding buffer (1 mM ß-mercaptoethanol). The lysate was loaded on the column and the column was washed two times with a 5 ml binding buffer (1 mM ß-mercaptoethanol) before the protein was eluted. The flowthrough was collected in Eppendorf tubes (wash 1 and wash 2). Afterwards, the protein was eluted with 6 ml elution buffer (containing ß-mercaptoethanol). The elution was collected in three portions. The first 0.6 ml were collected (=Elute 1), then 2.4 ml (Elute 2), and at least 3 ml (Elute3). Elute 2 was found to be the protein-containing fraction. All steps were performed at room temperature.

3.2.4. Endotoxin-Removal via EndoTrap® blue

After regenerating the column with Regeneration buffer, the column was washed with 6 ml Equilibration buffer (20 mM Tris-HCl + 200 mM NaCl + 10% Glycerol + 0.1 mM $CaCl_2$). 0.1 mM $CaCl_2$ was added to the lysate before the lysate was applied to the column and collected. Afterwards the column was washed with Equilibration buffer. And the 1 ml was collected to

the lysate. The column was washed with 5 ml regeneration buffer and stored in 1 ml Regeneration buffer + 0.002% sodium azide.

3.2.5. Buffer exchange

The protein was then buffer-exchanged using a PD-10 column (GE Healthcare). The column was washed twice with 5 ml ddH_2O and then three times with 5 ml Tris-HCl (pH=7). The column was equilibrated with 10 ml 20 mM Tris-HCl + 200 mM NaCl +10% glycerol (pH=7). The protein was loaded on the column. Finally, the protein was eluted with 7 ml 20 mM Tris-HCl + 200 mM NaCl +10% glycerol (pH=7). Seven fractions, each 1 ml, were collected (PD10 1-7). The three fractions with the highest protein amount were pooled.

3.2.6. Concentration of the proteins

The pooled fractions were concentrated using 10 kDa molecular weight cut off concentrator (45 minutes at 2000 xg at 4°C). The protein concentration was measured using a Bradford assay. The fractions from the HIS Gravi Trap Column and the PD10 Column were analyzed by SDS polyacrylamide gel electrophoresis (12% gel).

3.2.7. Protein concentration determination

3.2.7.1. Bradford assay

Standard	ddH_2O	BSA 1 µg/ml	Final concentration
1	800 µl	0 µl	0 ng/µl
2	790 µl	10 µl	1 ng/µl
3	780 µl	20 µl	2 ng/µl
4	760 µl	40 µl	4 ng/µl
5	740 µl	60 µl	6 ng/µl
6	720 µl	80 µl	8 ng/µl
7	700 µl	100 µl	10 ng/µl

Table 14: BSA standard dilution

The BSA dilutions were used for standard curve preparation. The BSA was diluted in ddH_2O, and 15 µl of protein was diluted in 885 µl ddH_2O. A dispenser was used to add 200 µl Bradford Reagent, and the samples were vortexed. After a 20 minute incubation time the samples were vortexed again. Duplicates of 200 µl of each sample and 200 µl of each standard dilution sample were pipetted on a 96-well microplate. The plate was put on the shaker for 15 seconds. Absorbance was measured at 595 nm with a photometric plate reader.

3.2.7.2. Bicinchoninic acid (BCA) protein assay

Standard	Buffer	BSA 2 µg/ml	Final concentration
1	720 µl	80 µl	200 ng/µl
2	400 µl	400 µl S1	100 ng/µl
3	400 µl	400 µl S2	50 ng/µl
4	400 µl	400 µl S3	25 ng/µl
5	480 µl	320 µl S4	10 ng/µl
6	400 µl	400 µl S5	5ng/µl
7	400 µl	400 µl S6	2.5 ng/µl
8	480 µl	320 µl S7	1 ng/µl
9	400 µl	0 µl	0 ng/µl

Table 15: BSA standard dilution

Working reagent:
Working reagent was prepared by mixing 50 parts of Micro BCA Reagent MA and 49 parts Reagent MB with 1 part of Reagent MC (MA:MB:MC= 50:49:1)

A dilution series of standard protein BSA was prepared using complete lysis buffer for dilution. 125 µl of the standard solutions and duplicates of the samples (1:50 dilution) were applied to a 96-well plate. 125 µl working reagent was added and the plate was shaken for 30 seconds. The plate was sealed and incubated for 2 hours at 37°C. The plate was cooled down

to room temperature for 5 minutes. Absorbance was measured at 562 nm with a photometric plate reader.

3.2.8. Sodium dodecyl sulfate polyacrylamide gel electrophoresis (SDS-PAGE)

The gel cassette was assembled, and the separation gel solution was prepared. In order to obtain a straight surface, isopropanol was added on top of the poured separating gel. After a 30 minutes polymerization time isopropanol was decanted, and the stacking gel solution was added. The comb was then placed quickly. The stacking gel was let to polymerize for 30 minutes. The protein samples were then prepared. Sample buffer was added and the samples were heated for 5 minutes at 95°C. The samples were briefly spun. The gel was put into the electrophoresis chamber. A 1X electrophoresis buffer was poured into the apparatus, and the comb was removed. The samples and the protein ladder were loaded on the gel. The SDS-PAGE was carried out at 180 V for 50 minutes. The gels were stained with Coomassie blue staining solution for 30 minutes and destained with destaining solution until the background was clear.

3.2.9. Cell Lysate preparation for Western Blot

Four hundred thousand NIH3T3 cells per well were plated in a 12 well plate and incubated for 24 hours. TAT-SMN1 was added at different concentrations (1000 nM, 750 nM, 500 nM, 250 nM, 125 nM, 0 nM) and incubated for 8 hours or at different time points (15 minutes, 30 minutes, 1 hour, 2 hours, 8 hours, 12 hours, 24 hours) and. The supernatants were taken and stored at -80°C (later referred to as “medium −trypsin”). Cells were treated with 0.0005% trypsin for 10 minutes at 37°C, 5% CO_2. The reaction was stopped with culture media, and the supernatants were stored at -80°C (later referred to as “medium +trypsin”). Following that cells were lysed with complete lysis buffer and scratched from the wells. Then the lysates were incubated for 30 minutes on ice, and were subjected to three cycles of freezing and thawing. In the next step cells were centrifuged for 10 minutes at 10.000 xg, and the supernatants were transferred into new Eppendorf tubes. Protein concentration was measured using the BCA method. The lysates were stored at -80°C and used for Western Blot analysis.

3.2.10. Western Blot

The following antibodies were used for Western blot analysis.

Antibodies

- His-Tag Polyclonal Antibody, (1:1000, Cell Signaling, #2365)
- Anti-6X His tag® antibody, (1:1000, abcam, #ab9108)
- Monoclonal Antibody to HIV-1 TAT basic domain, (1:1000, ACRIS, #A07H02010A-031)
- His Tag antibody, (1:3000, biorbyt, #orb66653)
- 6-His Affinity Purified Antibody, (1:1000, QED, #18814)
- STREB MAB Classic conjugated to horseradish peroxidase, (1:1000, IBA, #1509-007)
- STREB MAB Classic conjugated to horseradish peroxidase (1:32000, IBA, #1509-007)
- Anti-alpha Tubulin antibody - Loading Control, (1:15000, Sigma-Aldrich, #ab4074)

The proteins were separated by sodium dodecylsulfate (SDS) gel electrophoresis and immunoblotted onto a nitrocellulose membrane. The chamber for Western blot was assembled as follows: The nitrocellulose membrane, the filter paper and the sponges were equilibrated in blotting buffer. The gel was put on the membrane and the filter paper was put on each side. The sponges were put on the outside **(Figure 6).**

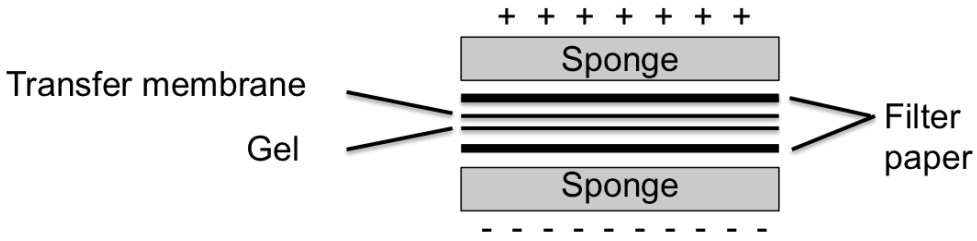

Figure 6: Western Blot assembly.

The blotting transfers of the proteins were performed for 35 minutes at 0.5 A at 4°C. After the transfer, the membrane was stained with Ponceau S (red), to make protein bands visible. The membrane was cut appropriately to get protein of interest on one membrane. In order to remove Ponceau S (red) the membrane was washed with 1X PBS until no red color was visible anymore. The membrane was blocked with blocking solution for 1 hour under gentle shaking. Then the membrane was either incubated overnight at 4°C with the primary antibody

against tubulin on a shaker, or protein bands were visualized with StrepMAB-Classic conjugated to horseradish peroxidase. The membrane was washed with 1X PBS. Substrate was added and incubated for 5 minutes and scanned on ChemiDoc™ Touch Gel Imaging System. The other part of the membrane had been incubated with secondary antibody for 1 hour and then washed with PBS. Substrate was added and incubated for 5 minutes and scanned on ChemiDoc™ Touch Gel Imaging System.

3.2.11. Test of protein stability

The extent of TAT-SMN1 protein degradation was obtained by determining the protein concentrations at different time points (0 hours, 24 hours, 48 hours, 72 hours) by Bradford assay. The protein was stored at 37°C and 5% CO_2 between the measurements.

3.2.12. Cell proliferation assay

The EZ4U kit (Biomedica) was used for the cell proliferation assay. In the manual provided by Biomedica (n.d.) the method is explained as follows:

> In 1956, the first paper was published on the use of tetrazolium salts as indicators of cell viability. The method was based on the finding that living cells are capable to reduce slightly or uncolored tetrazolium salts into intensely colored formazan derivatives. This reduction process requires functional mitochondria, which are inactivated within a few minutes after cell death. This method therefore provides an excellent tool for the discrimination of living and death cells.

Three thousand NIH3T3 cells per well were incubated overnight in a 96-well plate and treated with different TAT-SMN1 concentrations (1000 nM, 750 nM, 500 nM, 250 nM, 125 nM, 0 nM) for 4 hours at 37°C and 5% CO_2. Substrate was dissolved in 2.5 ml activator. The medium was removed, and a 20 µl substrate was added and incubated for 5 hours. Absorbance was measured at 450 nm.

3.2.13. Testing the effect of various trypsin concentrations on TAT-SMN1 transduction into NIH3T3 cells

To determine the trypsin concentration needed for the assay, different trypsin concentrations were tested. Overnight, 75,000 NIH3T3 cells were grown and then treated with different trypsin concentrations for 10 minutes. The reaction was stopped with Dulbecco's modified Eagle's medium (DMEM). The used trypsin concentrations were 0.001%, 0.0005%, and

0.000025% trypsin (diluted in PBS). Cells treated with 0.001% trypsin detach from the surface. No significant difference between cells treated with 0.0005% trypsin and cells treated with 0.000025% trypsin was observed. The higher of the two concentrations was used for further experiments.

3.2.14. Transduction and detection by indirect immunofluorescence

NIH3T3 cells were plated (200.000 cells/chamber in 500 µl) and incubated overnight at 37°C, 5% CO2. Cells were washed by adding medium and removing it. Cells were transduced with 500 nM TAT-SMN1 and incubated for 5 hours. NIH3T3 Cells were treated with 0.0005% Trypsin-EDTA for 10 minutes. The trypsinisation was stopped with a 500 µl medium. The medium was removed, and the cells were washed with ice-cold PBS. The cells were fied using 400 µl paraformaldehyde and were incubated for 15 minutes on ice. After fixation, cells were washed three times with ice-cold PBS. Then the cells were permeabilized by adding 300 µl ice cold 100% ethanol and incubated for 10 minutes on ice. Cells were blocked for 1 hour on a shaker with a blocking solution. After blocking cells were washed five times with 1X PBS and the primary antibody was diluted 1:200 in 1% BSA in PBS and incubated overnight at 4°C. The cells were washed five times and the secondary antibody was diluted to 1:250 and incubated for 1 hour in the dark. The cells were washed five times with 1X PBS. Diluted 4,6-Diamidine-2-phenylindole dihydrochloride (DAPI) was then and added to the cells. The cells were incubated for 10 minutes in the dark. The cells were then washed with 1X PBS and rinsed with ddH_2O. The attached chambers were removed. The coverslides were sealed with Fluoroprep.

3.3. Cell maintenance

3.3.1. NIH3T3 cells

NIH3T3 cells were cultivated in Dulbecco's Modified Eagle's Medium (DMEM) + 10% Fetal Bovine Serum (FBS) + 1% penicillin-streptomycin at 5% CO_2 and 37°C. Cells were split three times at a ratio of 1:5 using 0.25% trypsin-EDTA.

3.3.2. NSC-34

NSC-34 cells were cultivated in DMEM + 10% FBS + 1% penicillin-streptomycin at 5% CO_2 and 37°C. Cells were split three times a week at a ratio of 1:4 using 0.25% trypsin-EDTA.

3.3.3. Thawing of cells

Cells were thawed in a water bath at 37°C. Then the cells were re-suspended with medium and centrifuged at 500 xg for 7 minutes. The pellet was re-suspended in the medium, and the cells were transferred drop by drop into a cultivation flask. Cells were cultured at 37°C and 5% CO_2.

3.3.4. Freezing of cells

Cells were trypsinized using trypsin-EDTA. The reaction was then stopped with culture media. Cells were counted and centrifuged for 7 minutes at 250 xg, and 2.5×10^6 cells were re-suspended in culture medium + 10% Dimethylsulfoxid (DMSO). Cells were transferred to cryovials and frozen at −80°C. After 24 hours, the cells were transferred to liquid nitrogen container.

3.3.5. Cell splitting

The medium was removed, and the cells were washed with 1X PBS. The cells were treated for 2 minutes with trypsin-EDTA. Then the reaction was stopped with culture media. The cells were transferred partly into a new culture flask.

.

4. Results

4.1. Purification of TAT-SMN1 protein

E. coli pellets were solubilized using lysis buffer containing 8 M urea. For the purification of TAT-SMN1 protein, the lysate was applied to a Ni-affinity chromatography column for purification of histidine-tagged proteins. **(Figure 7A)**. After His-Tag purification the urea containing buffer was removed by applying the lysate to a desalting column. Two buffers for the desalting column were tested **(Figure 7B)**:

- 200 mM Tris/HCl, 10% glycerol and 0.1 mM EDTA, pH=7 (EB1);
- 200 mM Tris/HCl, 200 mM NaCl, 10% glycerol, pH=7 (EB2).

The flowthrough, wash 1, wash 2, elute 1 and elute 2 from TAT-SMN1 purification and the fractions from the desalting column were subjected to electrophoresis on a 12% polyacrylamide gel. The band for the concentrated protein at approximately 38 kDa is much stronger for the protein purified using EB2. The protein eluted with EB1 cannot be detected **(Figure 7C)**.

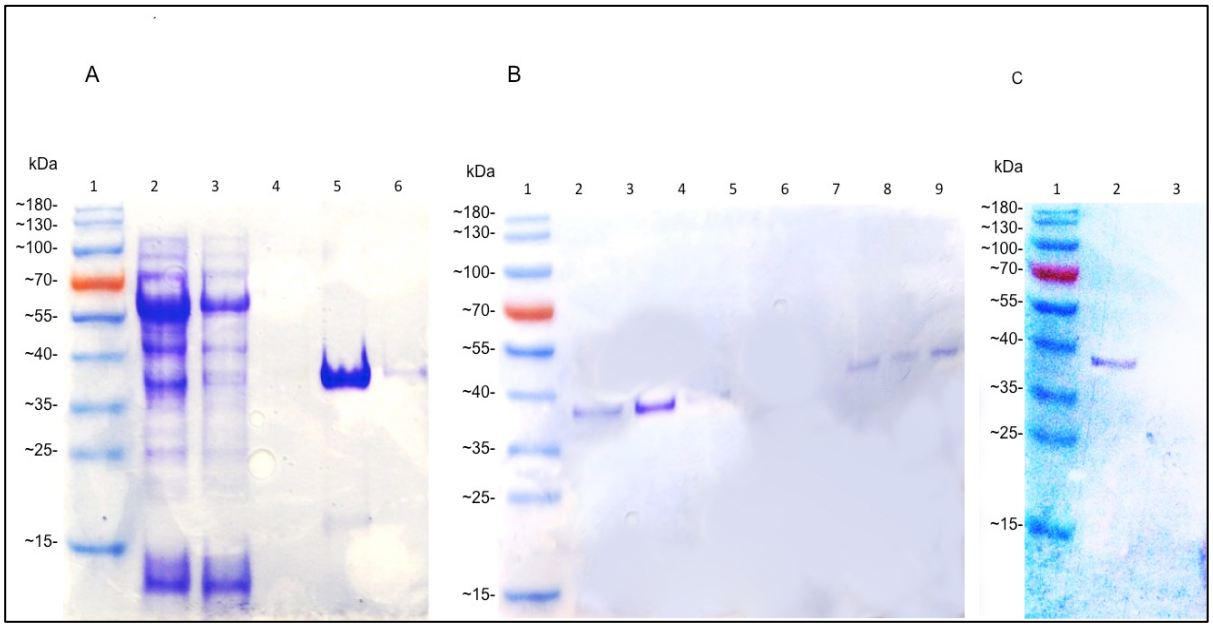

Figure 7: Effect of two different buffers on purification of TAT-SMN1 protein. A: 1: protein ladder. protein was purified using a HIS Gravi Trap column (GE Healthcare). 2: Flowthrough after HIS Gravi Trap column, 3: Wash 1, 4: Wash 2, 5: Elution 1: (1.5 ml), 6: Elution 2 (1 ml). **B:** Two buffers for the PD-10 column were tested. 200 mM Tris/HCl, 200 mM NaCl, 10% glycerol, pH=7 (2-5) and 200 mM Tris/HCl, 10% Glycerol and 0.1 mM EDTA, pH=7 (6-9). Samples from different fractions after PD-10 column subjected to electrophoresis on a 12% polyacrylamide gel. Gel was stained with Coomassie blue for 30 minutes. 2-5: Fractions from PD-10 column equilibrated with 200 mM Tris/HCl, 200 mM NaCl, 10% Glycerol, pH=7. 6-9: Fraction from PD-10 column equilibrated with 200 mM Tris/HCl, 10% Glycerol and 0.1 mM EDTA, pH=7. **C:** Fraction 2-5 from PD 10 column were pooled and concentrated using 10 kDa molecular weight cut off. For protein in 200 mM Tris/HCl, 200 mM NaCl, 10% Glycerol, pH=7, a band shows at approximately 38 kDa. TAT-SMN levels 200 mM Tris/HCl, 10% Glycerol and 0.1 mM EDTA, pH=7 are much lower, as no band is observed. Therefore 200 mM Tris/HCl, 200 mM NaCl, 10% Glycerol, pH=7 was used for further experiments.

4.1.1. Endotoxin removal

The endotoxins of the buffer-exchanged and pooled lysate fractions were removed by affinity chromatography. **Figure 8A** outlines the steps involved. The intensity of the band after endotoxin removal is much weaker, which indicates that a significant amount of protein is lost in the Endotrap column. The fractions were pooled and concentrated using 10 kDa molecular weight cut off concentrator **(Figure 8B)**. For further experiments, the endotoxin removal was left out in order to achieve higher protein concentrations.

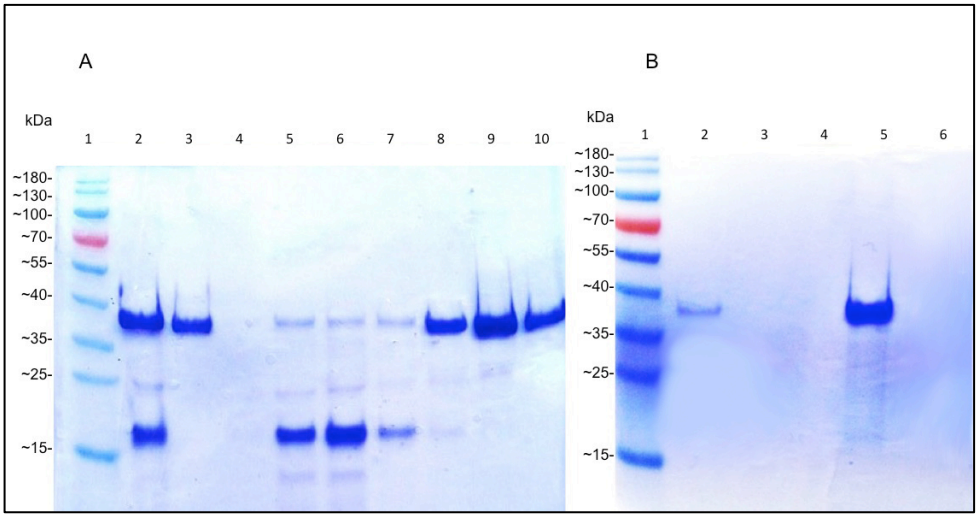

Figure 8: Endotoxin removal in the course of TAT-SMN1 protein purification. A: 1: Protein ladder. 2-3: protein was purified using a HIS Gravi Trap column (GE Healthcare). The second band at approximately 16 kDa is probably a host cell protein, present due to insufficient washing step. 4-10: In order to remove the urea containing buffer, the lysate was run on a PD-10 column equilibrated with 200 mM Tris/HCl, 200 mM NaCl, 10% Glycerol, pH=7. Samples from different fractions after PD10 column subjected to electrophoresis on a 12% polyacrylamide gel. Gel was stained with Coomassie blue for 30 minutes. The second band becomes almost invisible in PD-10 fractions 5-7 (8-10). **B:** 1: Protein ladder. 2: Endotoxin removal. The previously desalted and pooled lysate fractions were loaded on an Endotrap Blue column (Hyglos). 3: Equilibration buffer flowthrough of Endotrap column. 4: Regeneration buffer flowthrough of Endotrap column. When compared to the band in lane 1 with the fractions after the PD-10 desalting column, the band after endotoxin removal is much weaker, both due to protein dilution and sample loss during this process. 5: Concentrated protein using 10 kDa molecular weight cut off concentrator. SDS-PAGE was performed using a 12% polyacrylamide gel; protein(s) were visualized using Coomassie blue staining

4.1.2. Summary

In the first step, the protein was purified from cell lysate via Ni-affinity chromatography **(Figure 9A)**. In the next steps, the 8 M urea buffer was removed by a desalting column. The desalting column was equilibrated with 200 mM Tris/HCl, 200 mM NaCl, 10% glycerol, pH=7 **(Figure 9B)**. The fractions were pooled and concentrated using 10 kDa molecular weight cut off concentrator **(Figure 9C).**

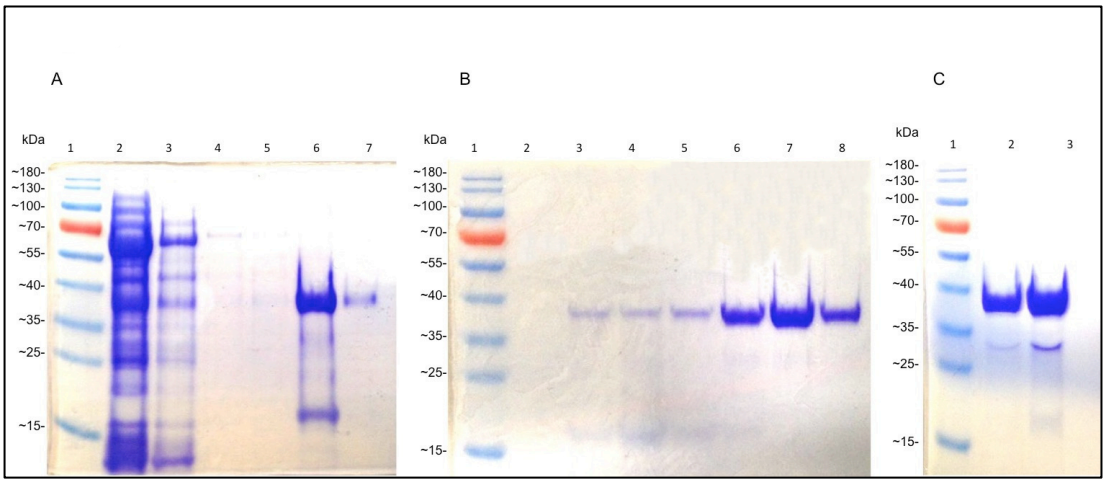

Figure 9: Purification of TAT-SMN1 protein. A: 1: Protein ladder. The next lanes show TAT-SMN purified using a HIS Gravi Trap column (GE Healthcare). 2: Flowthrough after HIS Gravi Trap column, 3: Wash 1, 4: Wash 2, 5: Elution 1: (0.6 ml), 6: Elution (2.4 ml), 7: Elution 3 (3 ml). Samples subjected to electrophoresis on a 12% polyacrylamide gel. Gel was stained with Coomassie blue. **B:** 1: Protein ladder. 2-10: In order to remove the urea containing buffer, the lysate was run on a PD-10 column equilibrated with 200 mM Tris/HCl, 200 mM NaCl, 10% Glycerol, pH=7. **C:** 1 protein ladder. 2: Fraction 5.6 and from PD 10 column were pooled. 3: Concentrated and pooled fractions. The small second band at approximately 30 kDa is probably due to contamination of PD-10 column. Samples were subjected to electrophoresis on a 12% polyacrylamide gel. Gel was stained with Coomassie blue.

4.2. Transduction and detection by indirect immunofluorescence

4.2.1. Testing the effect of various trypsin concentrations on TAT-SMN1 transduction into NIH3T3 cells

In order to avoid a false negative signal of protein that sticks on the cell surface, trypsin was used to remove possible protein from the cell surface. Various trypsin concentrations were tested. Cells treated with 0.001% trypsin were detaching from the surface. No significant difference between cells treated with 0.0005% trypsin and cells treated with 0.000025% trypsin was observed. The higher of the two concentrations was used for further experiments **(Figure 10).**

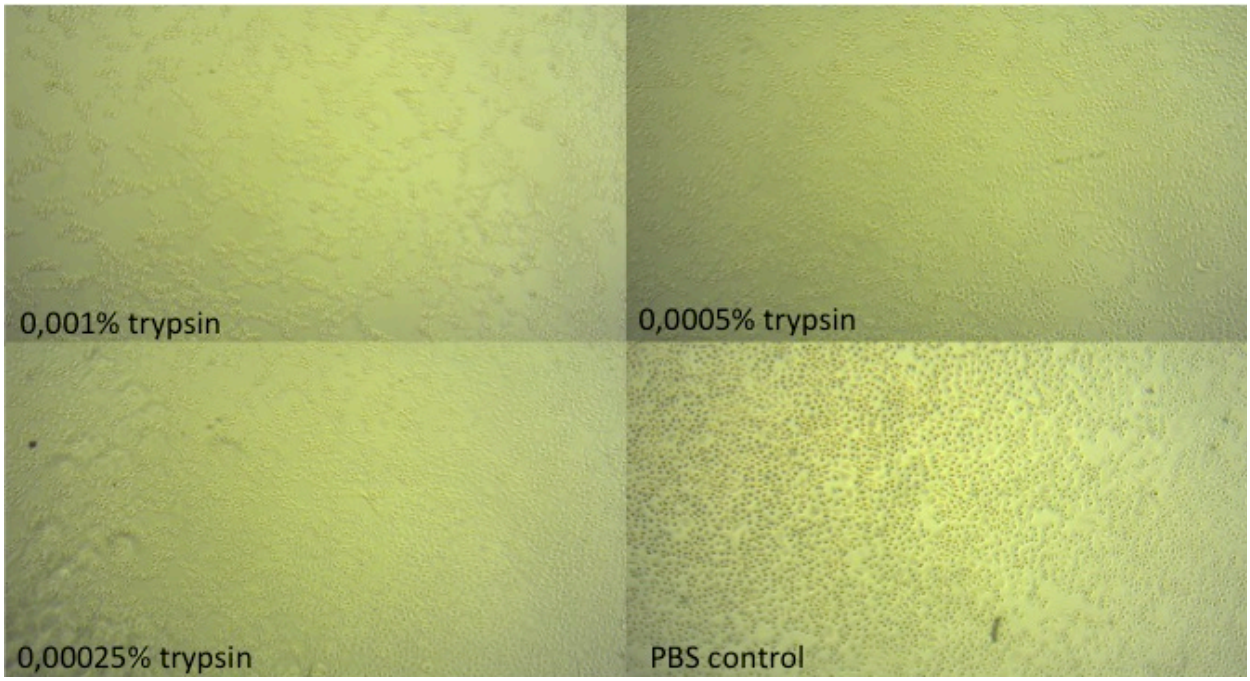

Figure 10: Effect of various trypsin concentrations on NIH3T3 cells. NIH3T3 cells were grown overnight and treated with various trypsin concentrations for 10 minutes. In the 0.001% trypsin panel many cells were removed after treatment. 0.0005% trypsin was used for further experiments.

4.2.2. Detection of HIS antibody by indirect immunofluorescence

The primary antibody was diluted 1:100 in 1% BSA in PBS. The secondary antibody was diluted to 1:250. Cell nuclei were labeled with DAPI. There is not much difference between the images of cells treated with trypsin and their untreated counterparts **(Figure 11 A/B)**. It seems therefore that TAT-SMN1 is present in the cell nuclei, but there is still a possibility that the detected protein is not in the nuclei, but is rather the surface. There is also a high degree unspecific binding in the untreated cells **(Figure 11D)**. In the next experiments we tried out Strep MAB Classic antibody, due to strong unspecific binding of His-Tag polyclonal antibody. A new staining procedure was devised and *z*-stack images of the cells were taken.

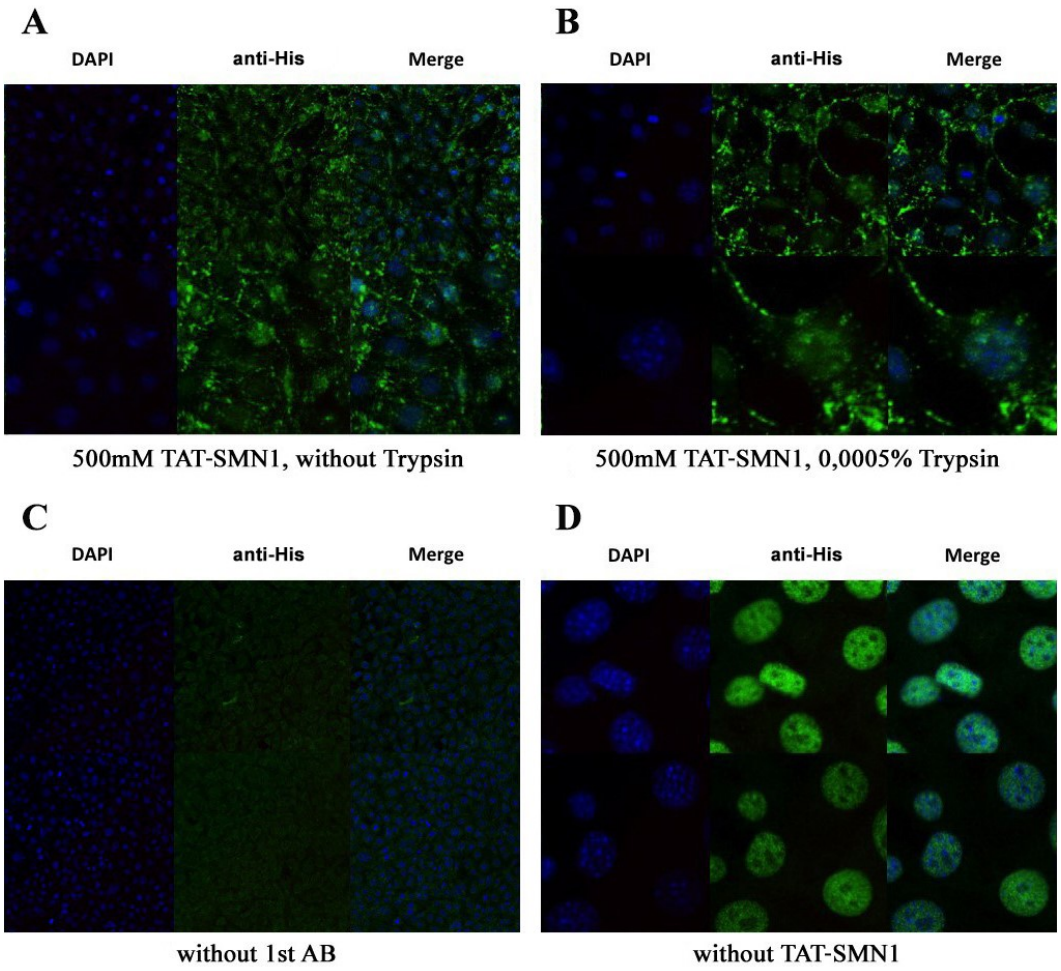

Figure 11: Localization of TAT-SMN1 in NIH3T3 cells. NIH3T3 cells were grown over night and incubated with 500 nM TAT-SMN1. Immunofluorescence staining of TAT-SMN1 (His-Tag polyclonal antibody followed by Alexa Fluor 488 secondary antibody. Cell nuclei were visualized by DAPI (4.6-diamidino-2-phenylindole). Magnification under the fluorescence microscope: It seems that TAT-SMN1 is in the cell nuclei, but from the images it was still unclear whether the protein sticks to the cell or is in the cell. There is much unspecific binding in untreated cells **(D)**. A new staining was done, and *z*-stack images of the cells were taken.

4.2.3. Detection of Strep antibody by indirect immunofluorescence

The primary antibody was diluted 1:200 in 1% BSA in PBS. The secondary antibody was diluted 1:250. The cell nuclei were labeled with DAPI. The *z*-stack series of cells was taken. It seems that a small amount of TAT-SMN1 is in the cell nuclei, and most of the protein is around the cell nuclei **(Figure 12).**

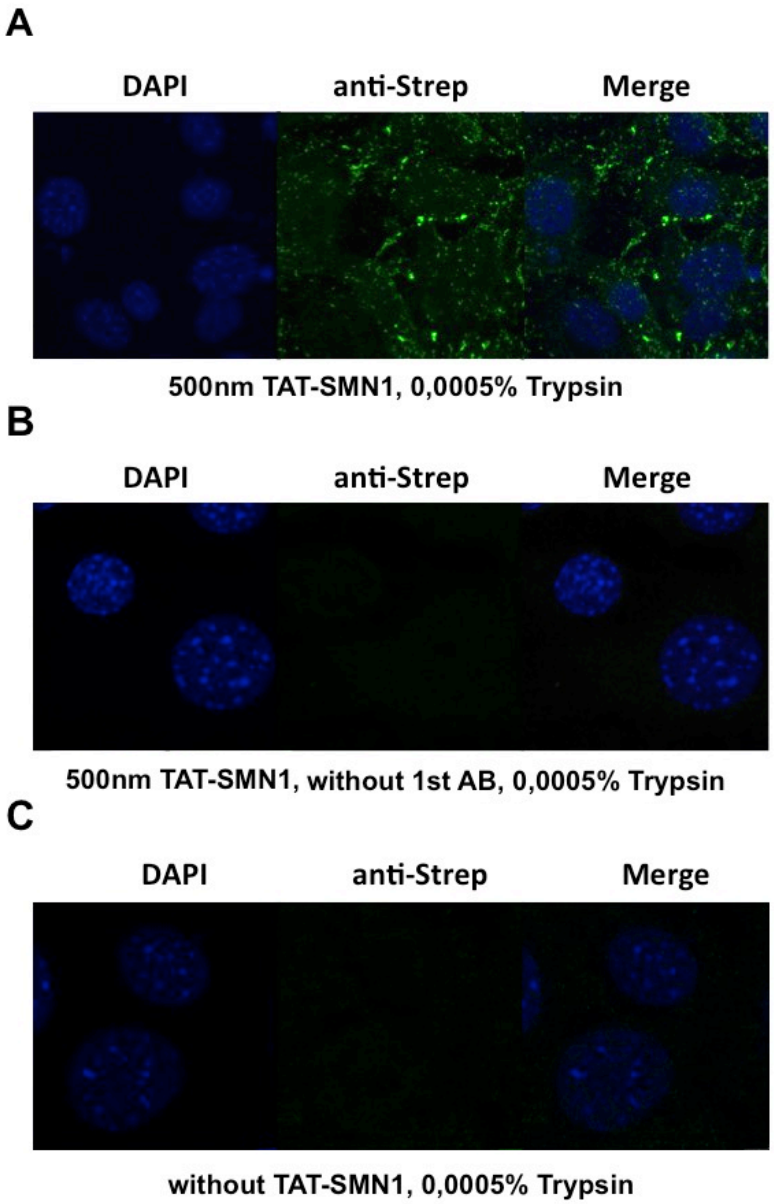

Figure 12: *Z*-stack series of NIH3T3 cells treated with TAT-SMN1. NIH3T3 cells were grown overnight and transduced with 500 nM TAT-SMN1 for 5 h. Cells were treated with 0.0005% trypsin before detection. Immunofluorescence staining of TAT-SMN1 (Strep MAB Classic antibody followed by Alexa Fluor 488 secondary antibody. Cell nuclei were visualized by DAPI (4.6-diamidino-2-phenylindole). **A:** DAPI panels: DAPI (4.6-diamidino-2-phenylindole) stained cell nuclei. Anti-Strep panels: TAT-SMN1 labeled with antibody against the Strep-tag of TAT-SMN1. Merge panels: merged images of DAPI (4.6-diamidino-2-phenylindole) stained cell nuclei and TAT-SMN1 labeled with antibodies against the Strep-tag. There seems to be a small amount of TAT -SMN1 in some of the cell nuclei. **B:** Negative control without 1st antibody. Only DAPI stained cell nuclei visible. **C:** Negative control of untreated NIH3T3 cells. There is some unspecific signal for anti-Strep.

4.2.4. Co-detection of Gemin3 antibody and Strep MAB classic antibody by indirect immunofluorescence

NIH3T3 cells were double stained with a SMN antibody and a gemin3 antibody. Gemin3 is known to colocalize with SMN1 in the cell. The gemin3 signal is very strong. This is probably due to too high concentration of the antibody. **Figure 13A** shows gemin3 distribution, without TAT-SMN1. TAT-SMN1 seems to stick on the cell surface or between the cells **(Figure 13B).** Gemin3 is localized to the cell nuclei. In the untreated cells, the signal for gemin3 is unchanged compared to those treated with TAT-SMN1. There is still some unspecific signal for TAT-SMN1 in the *z*-stack series **(Figure 13C).** The cells that were not treated with primary antibodies show no signal for TAT-SMN1 or gemin3 **(Figure 13D).**

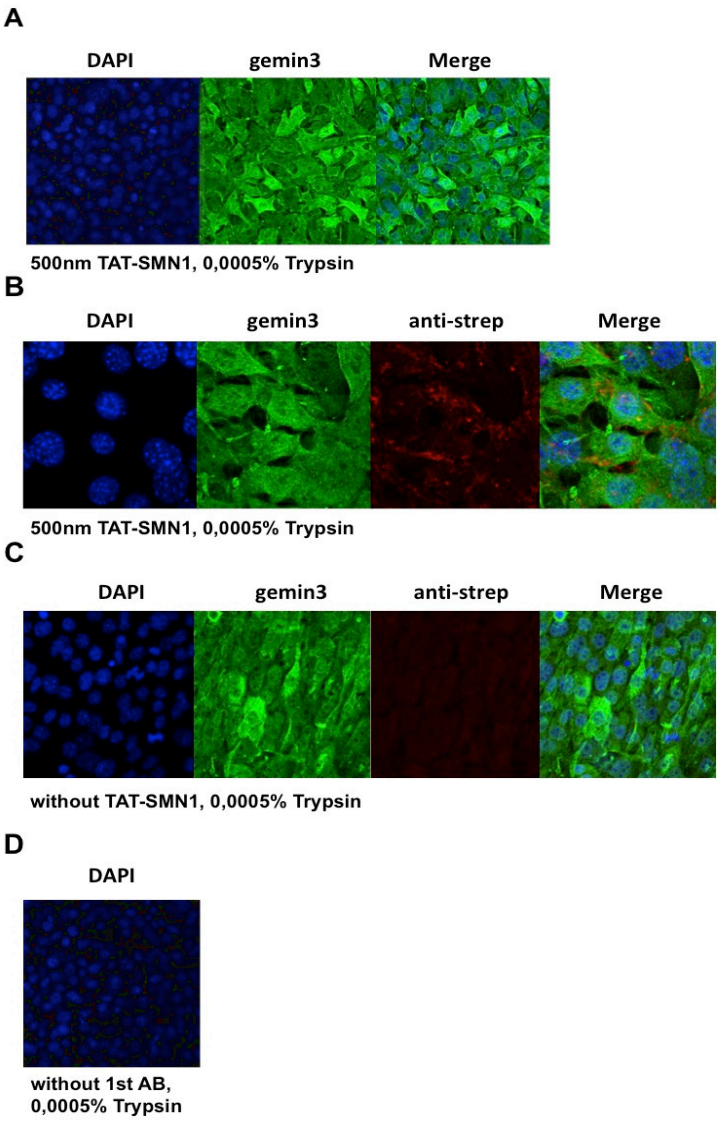

Figure 13: Co-detection of Gemin3 antibody and Strep MAB classic antibody by indirect immunofluorescence. *Z*-stack image of NIH3T3 cells that were treated with 500 nM TAT-SMN1 for 4 hours and with 0.0005% trypsin before detection. Immunofluorescence staining of TAT-SMN1 (Strep MAB Classic antibody followed by Alexa Fluor 568 secondary antibody) and Gemin3 (Gemin 3 antibody followed by Alexa Fluor 488 secondary antibody). Cell nuclei were visualized by DAPI (4.6-diamidino-2-phenylindole). DAPI panel: DAPI stained cell nuclei. TAT-SMN1 panel: TAT-SMN1 labeled with antibodies against Strep-tag. Gemin3 panel: Gemin labeled with antibodies against Gemin3. Merge panel: merged images of DAPI (4.6-diamidino-2-phenylindole) stained cell nuclei and TAT-SMN1 labeled with antibodies against Strep-tag and gemin labeled with antibodies against Gemin3. Magnification under the fluorescence microscope:. **A**: Immunofluorescence staining Gemin3. Gemin3 was localized in the cell nuclei. **B:** Immunofluorescence staining of TAT-SMN1 (and Gemin3. The Gemin3 signal is very strong. TAT-SMN1 seems to stick on the cell surface or between the cells. **C:** Negative control of untreated NIH3T3 cells. Signal for Gemin3 is strong. Unspecific signal for TAT-SMN1. **D**: Negative control without 1st antibodies. No signal for Gemin3 or Strep MAB classic.

4.2.5. Co-detection of SMN antibody and Strep MAB classic antibody by indirect immunofluorescence

NIH3T3 cells were also double stained with STREP Antibody and SMN antibody. The SMN can be found in the cytoplasm and the nuclei of cells. A *z*-stack series of composite emissions from Alexa Fluor 488 and Alexa Fluor 568 and DAPI was taken.

There is a very strong signal for SMN and for TAT-SMN1. In the merge of the *z*-stack series, the yellow color indicates that both proteins colocalize in the cell nuclei and cytoplasm **(Figure 14B).** The signal for TAT-SMN1 is very strong compared to previous experiments. This is probably due to unspecific binding of secondary antibody.

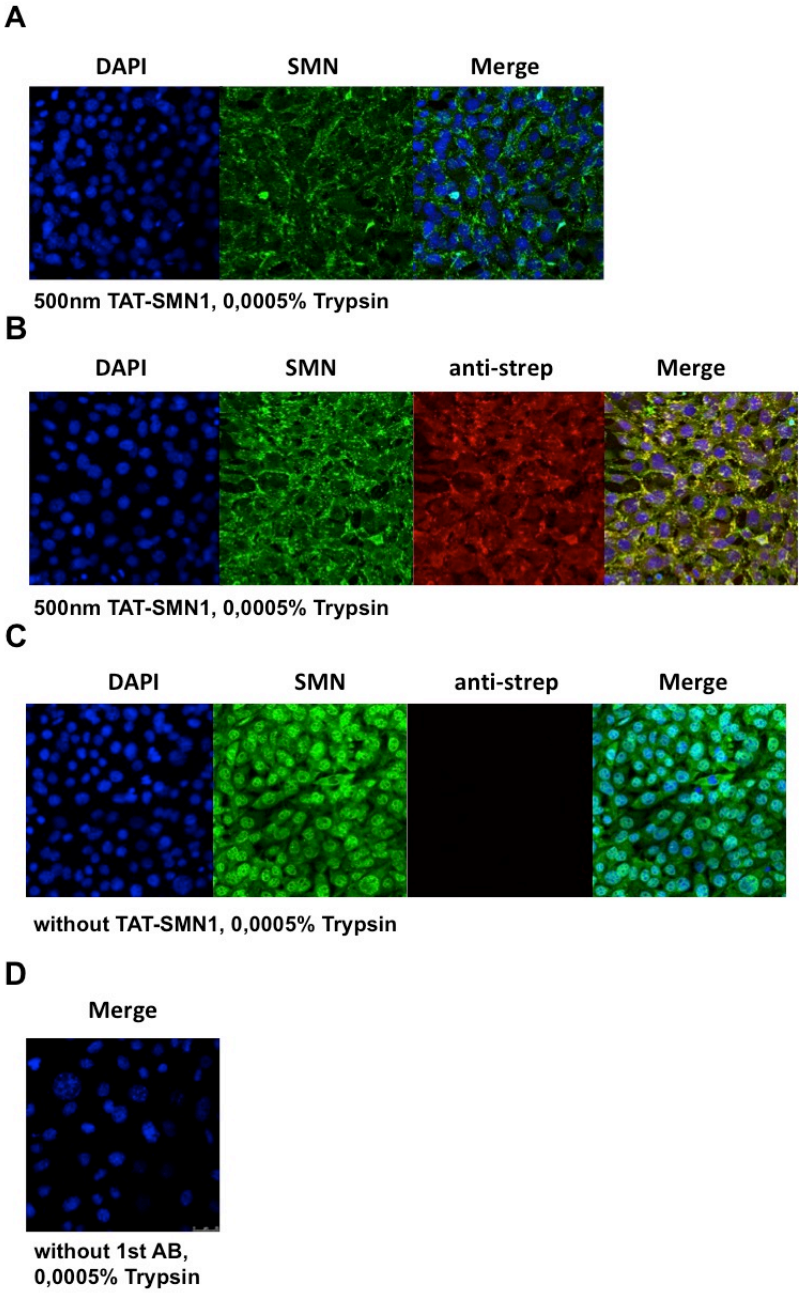

Figure 14: Co-detection of SMN antibody and Strep MAB classic antibody by indirect immunofluorescence. *Z*-stack image of NIH3T3 cells, that were treated with 500 nM TAT-SMN1 for 4 hours and with 0.0005% trypsin before detection. Immunofluorescence staining of TAT-SMN1 (Strep MAB Classic antibody followed by Alexa Fluor 568 secondary antibody) and SMN (SMN antibody followed by Alexa Fluor 488 secondary antibody). Cell nuclei were labeled with DAPI (4.6-diamidino-2-phenylindole). DAPI panel: DAPI (4.6-diamidino-2-phenylindole) stained cell nuclei. SMN panel: SMN labeled with antibodies against SMN. Anti-strep panel: TAT-SMN1 labeled with antibodies against strep-tag. Merge panel: merged images of DAPI (4.6-diamidino-2-phenylindole) stained cell nuclei and TAT-SMN1 labeled with antibodies against strep-tag and SMN labeled with antibodies against SMN. **A:** Immunofluorescence staining of SMN. **B:** Immunofluorescence staining of TAT-SMN1 and SMN. In the merge of the *z*-stack series the yellow colour indicates that both proteins colocalize in the cell nuclei and cytoplasm. **C:** Negative control of untreated NIH3T3 cells. Signal for SMN is strong, but there is almost no signal for TAT-SMN1. **D:** Negative control without 1st antibodies. No signal for SMN or Strep MAB classic.

4.2.6. Experiments with NSC-34 cells

4.2.6.1. Testing of various trypsin concentrations on TAT-SMN1 transduction into NSC-34 cells.

In order to avoid a signal from protein that sticks on the cell surface, trypsin was used to remove possibly adhering TAT-SMN1. Various trypsin concentrations were tested. One-hundred-fifty thousand NSC-34 cells were grown overnight and then treated with different trypsin concentrations for 10 minutes. The reaction was stopped with DMEM. The used trypsin concentrations were 0.001% trypsin, 0.000125% trypsin, 0.0000625% trypsin **(Figure 15)**. At 0.0000625% trypsin: some cell colonies detached, but most of the cells stick to the surface; therefore, 0.0000625% trypsin was used in the next experiments.

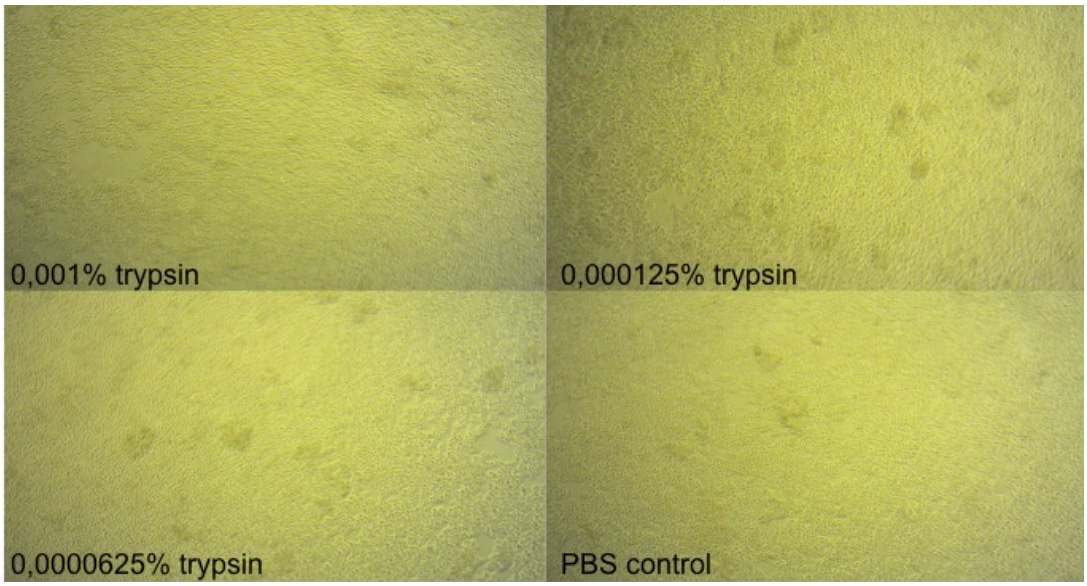

Figure 15: Effect of various trypsin concentrations on NSC-34 cells. NSC-34 cells were grown overnight and incubated with different trypsin concentrations for 10 minutes at 0.001% trypsin and 0.000125% trypsin: some cells detached. 0.0000625% trypsin: some cell colonies detached, but most of the cells stick to the surface; therefore, 0.0000625% trypsin was used in the next experiments.

4.2.6.2. Co-detection of Gemin3 antibody and Strep MAB classic antibody by indirect immunofluorescence

NSC-34 cells were double stained with a Strep antibody for TAT-SMN1 and a gemin3 antibody. There is very strong signal for gemin3. It is not clear from the images whether TAT-SMN1 enters the cell nuclei of NSC-34 **(Figure 16).**

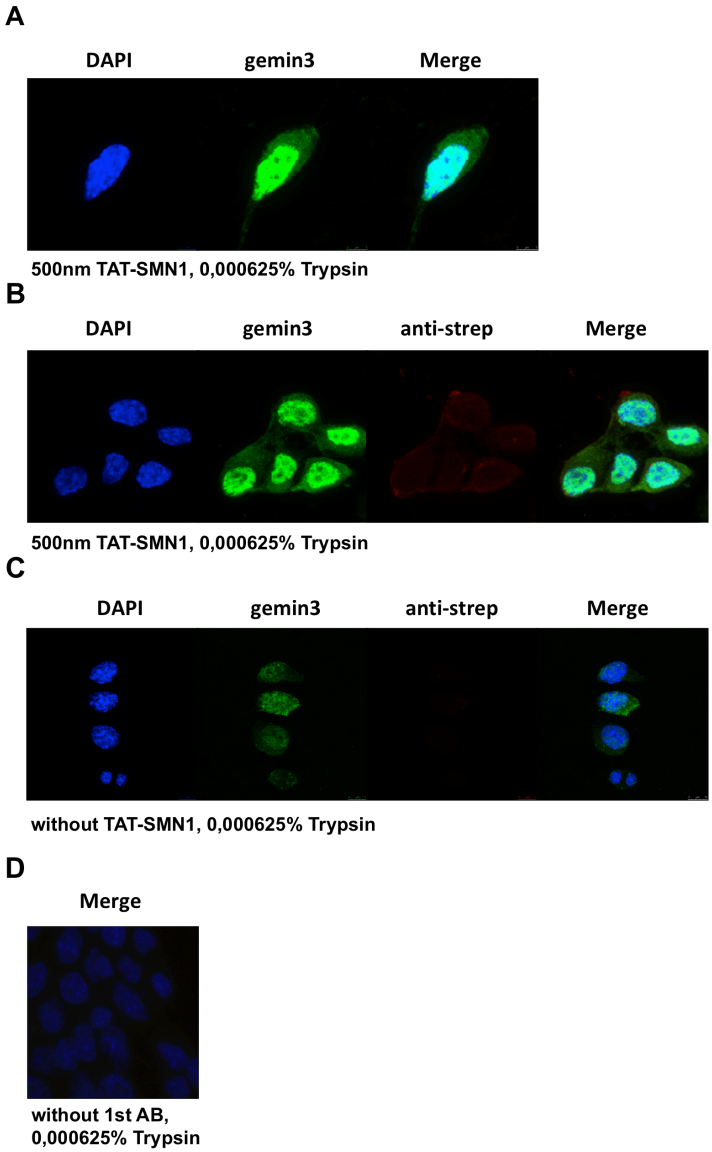

Figure 16: Co-detection of Gemin3 antibody and Strep MAB classic antibody by indirect immunofluorescence. 800000. NSC-34 cells were grown overnight. *Z*-stack image of NSC-34 cells were treated with 500 nM TAT-SMN1 for 4 hours and with 0.0000625% trypsin before detection. Immunofluorescence staining of TAT-SMN1 (Strep MAB Classic antibody followed by Alexa Fluor 568 secondary antibody) and Gemin3 (Gemin3 antibody followed by Alexa Fluor-488 secondary antibody). Cell nuclei were labeled with DAPI (4.6-diamidino-2-phenylindole). DAPI panel: DAPI 4.6-diamidino-2-phenylindole stained cell nuclei. Gemin3 panel: gemin labeled with Gemin3 antibody. TAT-SMN1 panels: TAT-SMN1 labeled with Strep Antibody. Merge panel: merged images of DAPI (4.6-diamidino-2-phenylindole) stained cell nuclei and TAT-SMN1 labeled with Strep Antibody and Gemin3 labeled with Gemin3 antibody. **A:** Immunofluorescence staining of Gemin3. **B:** Immunofluorescence staining of TAT-SMN1 and Gemin3. There is a very strong signal for Gemin3 antibody, almost none for Strep MAB Classic. It is not possible to draw conclusions about whether TAT-SMN1 is in the nuclei or not. **C:** Negative control of untreated NSC-34 cells. Signal for Gemin3 is strong and the signal for TAT-SMN1 is unspecific. **D:** Negative control without 1st antibodies. No signal for Gemin3 or Strep MAB classic.

The data shown above suggests that TAT-SMN1 goes into the cell nuclei of NIH3T3 after treatment with a certain concentration of purified TAT-SMN1. To confirm this hypothesis, a Western blot with TAT-SMN1 was performed.

The affinity of various antibodies for TAT-SMN1 was investigated: 7.75 nM and 15.5 nM TAT-SMN1 were tested for each antibody. A 12% SDS-PAGE was used for separation.
Tested antibodies:

- His-Tag Polyclonal Antibody, (1:1000)
- Anti-6X His tag® antibody, (1:1000)
- Monoclonal Antibody to HIV-1 TAT basic domain, (1:1000)
- His Tag antibody, (1:3000)
- 6-His Affinity Purified Antibody, (1:1000)
- STREB MAB Classic conjugated to horseradish peroxidase, (1:1000)
- STREB MAB Classic conjugated to horseradish peroxidase (1:32000)

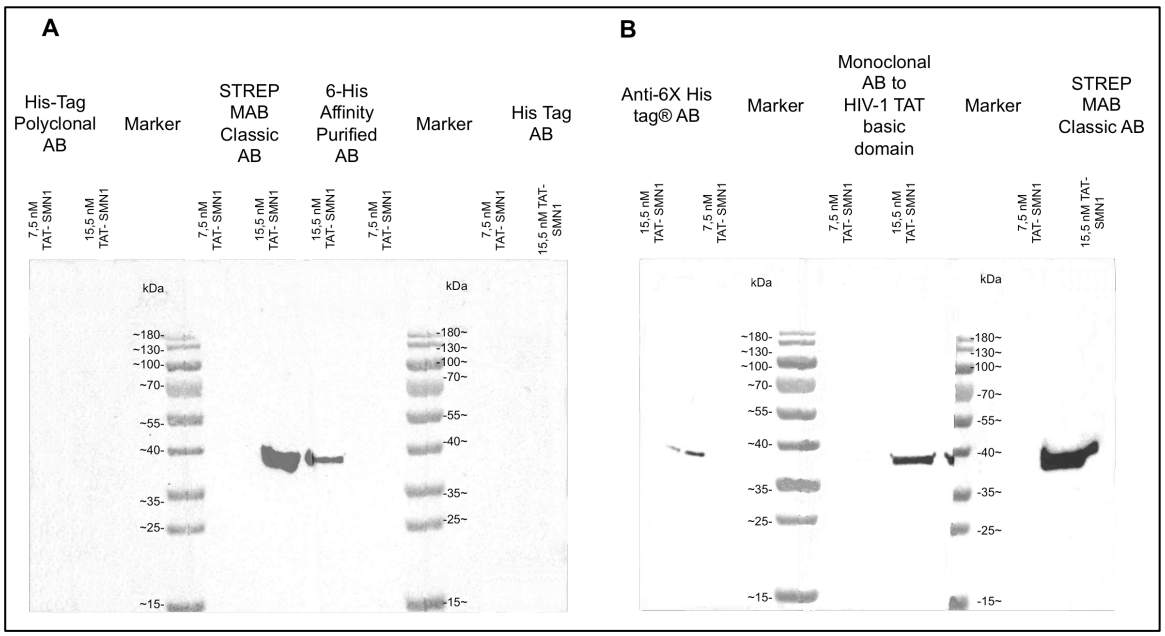

Figure 17: Affinity of different antibodies for TAT-SMN1. HIS TAG Polyclonal Antibody, cell signalling 2365: There is no protein band for this antibody. STREB MAB Classic conjugated to horseradish peroxidase (1:32000), IBA, 1509-007: There is a protein band at approximately 38 kDa for 15.5 nM TAT-SMN1. Anti 6X HIS tag antibody, Abcam, ab9108: A protein band at 38 ka for 1 nm TAT-SMN1 is visible. Mouse monoclonal to HIS TAG, biorbyt, orb66653: There is no protein band visible. B: Anti 6X HIS tag antibody, Abcam, ab9108: A small protein band at 38 ka for 15.5 nM TAT-SMN1 is visible. Monoclonal Antibody to HIV-1 TAT basic domain: There is a protein band at approximately 38 kDa 15.5 nM TAT-SMN1. STREB MAB Classic conjugated to horseradish peroxidase (1:1000), IBA, 1509-007: A strong protein band at 38 ka for 15.5 nM TAT-SMN1 is visible.

TAT-SMN1 is clearly detected with Strep MAB Classic (1:1000 dilution), so the subsequent experiments were carried out with Strep MAB Classic (1:1000 dilution).

4.2.7. Transduction of various TAT-SMN1 concentrations into NIH3T3 cells

Cells were treated with purified TAT-SMN1 protein. The media before and after trypsin treatment was collected. The lysate lane and the medium −trypsin should show a protein band. The medium +trypsin lane should not give rise to a signal band since it should be degraded by trypsin. Cells treated with 125 nM TAT-SMN1 showed no protein band at all. It is possible that one well with cells was left out during treatment with TAT-SMN1 or that the Eppendorf tube with TAT-SMN1 was not mixed properly, so the cells were not treated with a sufficient amount of TAT-SMN1. At 250 nM TAT-SMN1, protein could be detected in lysates and in the concentrated medium without trypsin control sample. The protein in the non-concentrated media seems to be too low for detection **(Figure 18A)**.

For 500 nM, 750 nM and 1000 nM TAT-SMN1, there is a protein band in the lysate sample and the medium –trypsin control as already expected. However, at 1000 nM there is also a light protein band in medium + trypsin sample. It is possible that due to the high TAT-SMN1 concentration, trypsin does not remove all of the protein, so a small remaining amount of TAT-SMN1 can still be detected **(Figure 18B).** For the next experiments, it was decided to also detect tubulin as a loading control.

Figure 19 shows a Western blot of previously with TAT-SMN1 treated cells. The NIH3T3 cells were treated with increasing TAT-SMN1 concentrations (0 nM, 125 nM, 250 nM) and lysed with complete lysis buffer. Protein concentration was measured using BCA assay. In the negative control, no TAT-SMN1 could be detected. There is a very strong signal for tubulin in the untreated cells. In cells treated with 125 nM TAT-SMN1 a strong band for tubulin was detected in the lysates, but no TAT-SMN1. In the –trypsin control, there was TAT-SMN1. For 250 nM TAT-SMN1, a strong band for tubulin was detected in lysate, but no TAT-SMN1 (probably due to imprecise cutting of the membrane) is found. TAT-SMN1 could be detected in medium −trypsin sample. This result could be due to imprecise cutting of the membrane.

In the Western blot of lysates of cells treated with 500 nM TAT-SMN1, tubulin was detected in the lysates. TAT-SMN1 was detected in the lysates and in the medium –trypsin control. The band for TAT-SMN1 is slightly stronger than the band for tubulin. In the lysates of cells treated with 750 nM we observed the same result, but there is a light band in the trypsin + medium lane. In 1000 nM TAT-SMN1, tubulin can be found in the lysates, but not TAT-SMN1. This is probably due to imprecise cutting of the membrane. TAT-SMN1 was detected in the trypsin-medium control **(Figure 19B).**

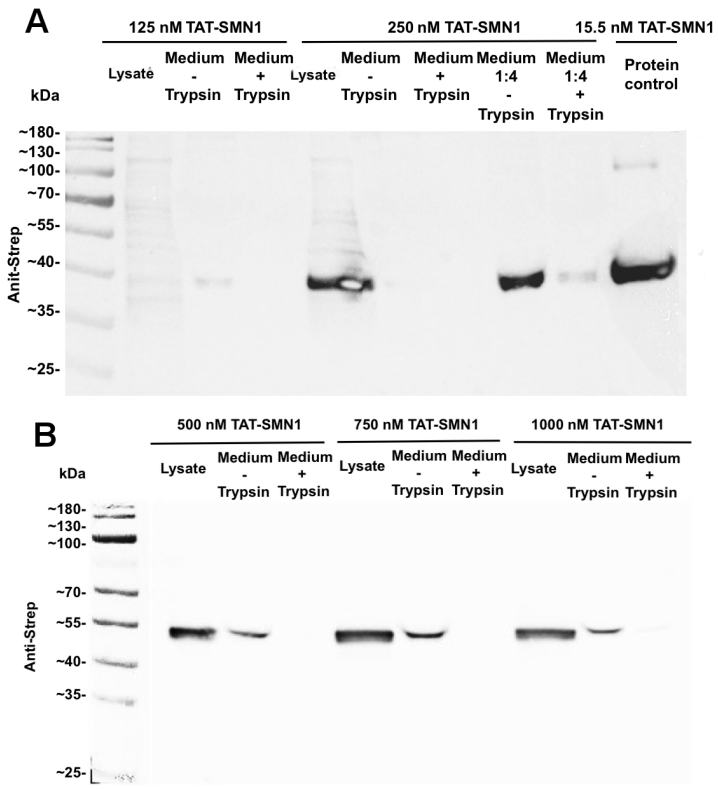

Figure 18: Transduction of various TAT-SMN1 concentrations into NIH3T3 cells. NIH3T3 cells were grown overnight, treated with different TAT-SMN1 concentrations for 4 hours, and lysed and separated by electrophoresis. The lysates were used for Western blot analysis**. A:** 125nM TAT-SMN1: No protein could be detected. 250 nM TAT-SMN1: A protein was detected in the lysate band. No protein detected in the non-concentrated medium samples. In 1:4 concentrated medium a protein band was detected in –trypsin control. 15.5 nM TAT-SMN1 control: strong protein band at approximately 38 kDa. **B:** 50 nM TAT-MN1 protein was detected in the lysate band and protein detected in the –trypsin control. As expected no protein was detected in the medium +trypsin lane. 750 nM: TAT-SMN1 protein was detected in the lysate band and protein was detected in the –trypsin control. As expected, no protein could be detected in medium +trypsin lane. 1,000 nM TAT-SMN1 protein was detected in the lysate band, and the protein was detected in the –trypsin control. The light protein band was detected in medium +trypsin lane.

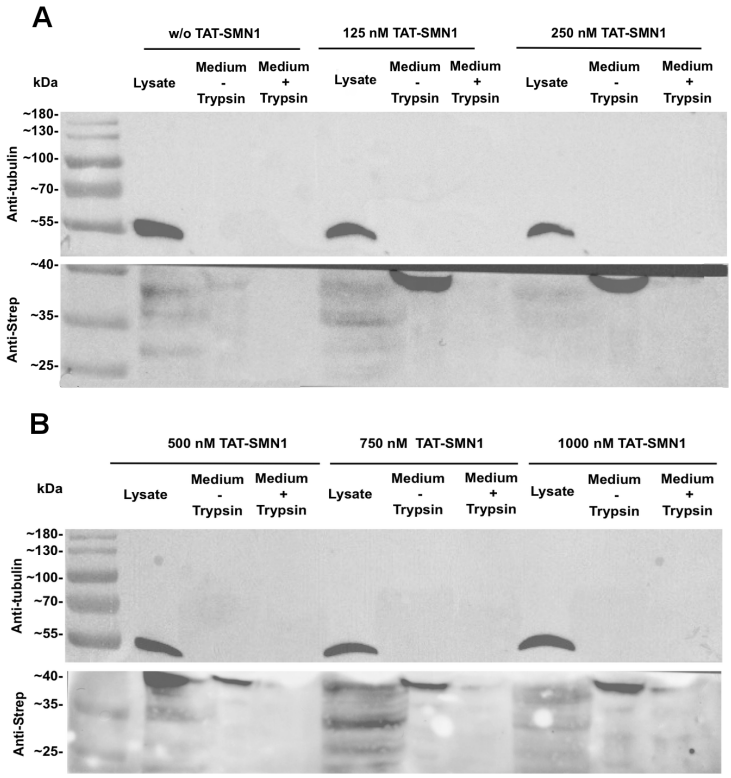

Figure 19: Transduction of various TAT-SMN1 concentrations into NIH3T3 cells. NIH3T3 cells were grown overnight, treated with different TAT-SMN1 concentrations for 4 hours, and lysed and separated by electrophoresis. The lysates were used for Western blot analysis. **A:** Without TAT-SMN1: tubulin was detected in lysate. No protein band for the other samples. 125 nM TAT-SMN1 tubulin was detected for lysate. No TAT-SMN1 detected in lysate, but in medium –trypsin control. 250 nM TAT-SMN1: tubulin was detected in lysate, but no TAT-SMN1 (probably due to wrong cutting of the membrane) in lysate, but in medium –trypsin TAT-SMN1 is present. **B:** 500 nM TAT-SMN1: Tubulin was detected in lysate. TAT-SMN1 protein was detected in the lysate band and protein was detected in the –trypsin control. As expected, no protein was present in medium +trypsin lane. 750 nM TAT-SMN1 tubulin was detected in lysate. TAT-SMN1 protein was detected in the lysate band and protein was detected in the –trypsin control. Light protein band in medium +trypsin lane. 1000 nM TAT-SMN1: Tubulin was detected in lysate. No TAT-SMN1 (probably due to wrong cutting of the membrane) in lysate, but in the medium –trypsin sample, a weak protein band at approximately 38 kDa in medium –trypsin control is observed.

4.2.8. Transduction of TAT-SMN1 into NIH3T3 cells for different time periods

The experimental setup was the same as in the concentration dependent experiments, except that all cells were treated with 500 nM TAT-SMN1 but at different time timespans. The expected result is the same as in concentration-dependent experiments, the lysate lane and the medium −trypsin lane should show a band at approximately 38 kDa. The medium + trypsin lane should not show a protein band, since protein gets degraded by trypsin. **Figure 20A** shows the Western blot for cells treated for 30 minutes and for 1 hour. After being treated for 30 minutes, TAT-SMN1 could be detected in the lysates and in the medium without trypsin sample. However, after 1 hour, there seems to be no TAT-SMN1 at all in the lysates. The small band in the medium +trypsin lane is probably spill-over from the 15.5 nM TAT-SMN1 control. That well was likely left out upon treatment. In **Figure 20B**, the cells treated for 2 hours show the expected result. There is TAT-SMN1 in the lysates and in the medium –trypsin sample. Yet for the cells treated for 8 hours, TAT-SMN1 was detected only in the lysates, but not in the medium –trypsin control. For the medium +trypsin, there is light band at 38 kDa, but this could also be a spill-over from the 15 nM TAT-SMN1 control.

Figure 21A shows the Western blot for cells treated for 15 minutes and for 1 hour. Both show that the lysate lane and the medium −trypsin lane should have a band at approximately 38 kDa. The medium +trypsin lane should not show a protein band, since protein gets degraded by trypsin. The same analysis can be applied for the samples in **Figure 21B** (4 hours, 24 hours).

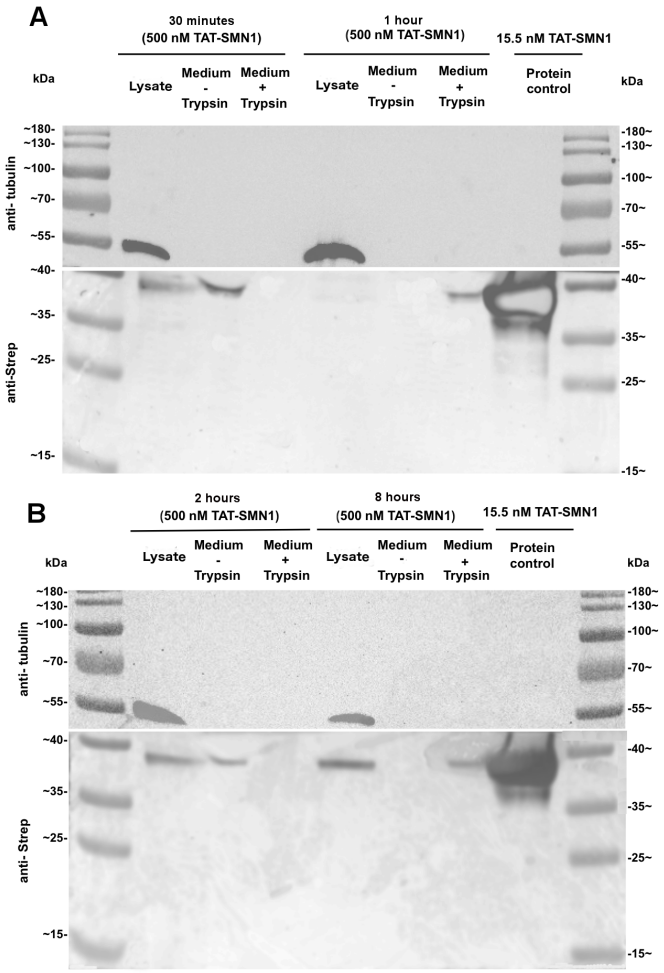

Figure 20: Transduction of TAT-SMN1 into NIH3T3 cells at different time points. NIH3T3 cells were grown overnight and treated with 500 nM TAT-SMN1 for different time spans and lysed and separated by electrophoresis. The lysates were used for Western blot analysis. **A:** 30 minutes: Tubulin was detected in in the lysate. TAT-SMN1 protein was detected in the lysate band and protein was detected in the –trypsin control. As expected no protein was detected in medium +trypsin lane. 1 hour: Tubulin was detected in the lysate, but No TAT-SMN1 was detected, except in the medium –trypsin lane (probably some of the sample from lane 9 spill over). 15.5 nM TAT-SMN1 control: No tubulin was detected. Strong TAT-SMN1 band is found. **B:** 2 hours: Tubulin was detected in lysate. TAT-SMN1 protein was detected in the lysate band and protein was detected in the –trypsin control. As expected no protein was detected in medium +trypsin lane. 8 hours: Tubulin was detected in lysate. TAT-SMN1 was detected in the lysate band, and no protein was detected in the –trypsin control. Small band was detected in medium +trypsin lane (probably some of the sample from 15.5 nM TAT-SMN1 control slop over). 15.5 nM TAT-SMN1 control: No tubulin was detected. Strong TAT-SMN1 band is present.

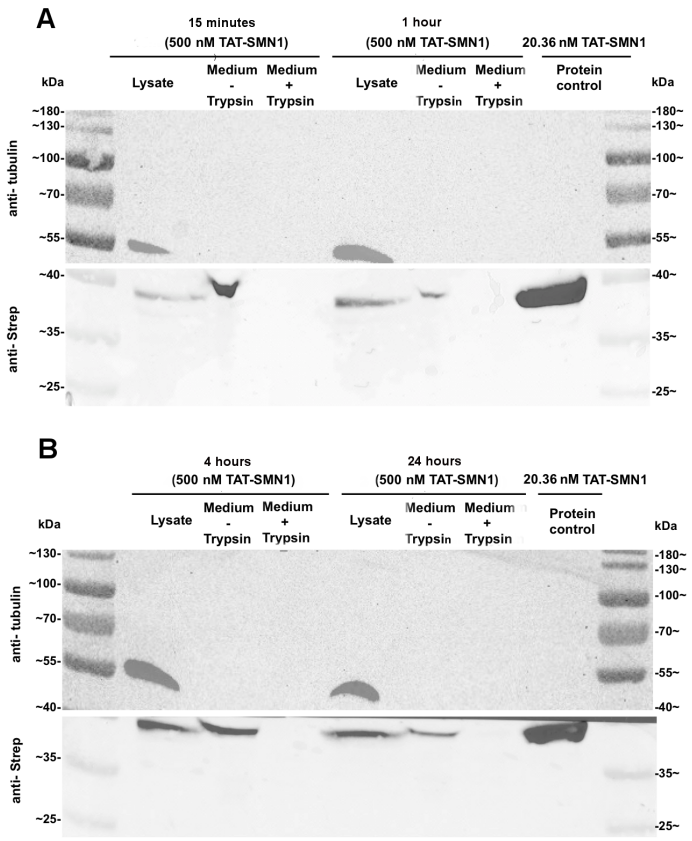

Figure 21: Transduction of TAT-SMN1 into NIH3T3 cells at different time points. NIH3T3 cells were grown overnight and treated with 500 nM TAT-SMN1 for different time spans and lysed and separated by electrophoresis. The lysates were used for Western blot analysis. **A:** 15 minutes: Tubulin was detected in lysate. TAT-SMN1 protein was detected in the lysate band and protein was detected in the –trypsin control. As expected no protein was detected in medium +trypsin lane. 1 hour: Tubulin was detected in lysate. TAT-SMN1 protein was detected in the lysate band and protein was detected in the –trypsin control. As expected no protein was detected in medium +trypsin lane. 20.36 nM TAT-SMN1 control: No tubulin was detected. Strong TAT-SMN1 band is seen. **B:** 4 hours: Tubulin was detected in lysate. TAT-SMN1 protein was detected in the lysate band and protein was detected in the –trypsin control. As expected no protein was detected in medium +trypsin lane. 24 hours: Tubulin was detected in lysate. TAT-SMN1 protein was detected in the lysate band and protein was detected in the –trypsin control. As expected no protein was detected in medium +trypsin lane. 20.36 nM TAT-SMN1 control: No tubulin was detected. Strong TAT-SMN1 band is present.

4.3. TAT-SMN1 Stability

TAT-SMN1 concentration was measured at different time points (0 hours, 24 hours, 48 hours, and 72 hours) by using the Bradford assay. The experiment was repeated with TAT-SMN1 from another batch.

In the first experiment, we can see a minor decline in the concentration of TAT-SMN1 until 48 hours, after that the concentration almost increases to the initial concentration **(Figure 22A)**. In the second experiment there seems to be an increase in the TAT-SMN1 concentration until 48 hours. After that concentration decreases to almost the initial value. The rise in the 48 hours may occur due to evaporation **(Figure 22B).**

There is either a small amount of TAT-SMN1 degradation or the differing concentration is due to fluctuations in the measurement process. The rise from 48 hours to 72 hours could again occur due to evaporation **(Figure 22B)**. Hence, it is possible that the different concentrations from the Bradford assay measurement might occur due to fluctuations during the measuring process **Figure 22C** summarizes both experiments and shows the degradation in percent. The concentration is very stable with almost no fluctuation. The samples from the first experiment were run on a 12% SDS-Page. The 0 hour band is slightly stronger than the bands for the other points in time **(Figure 22D).**

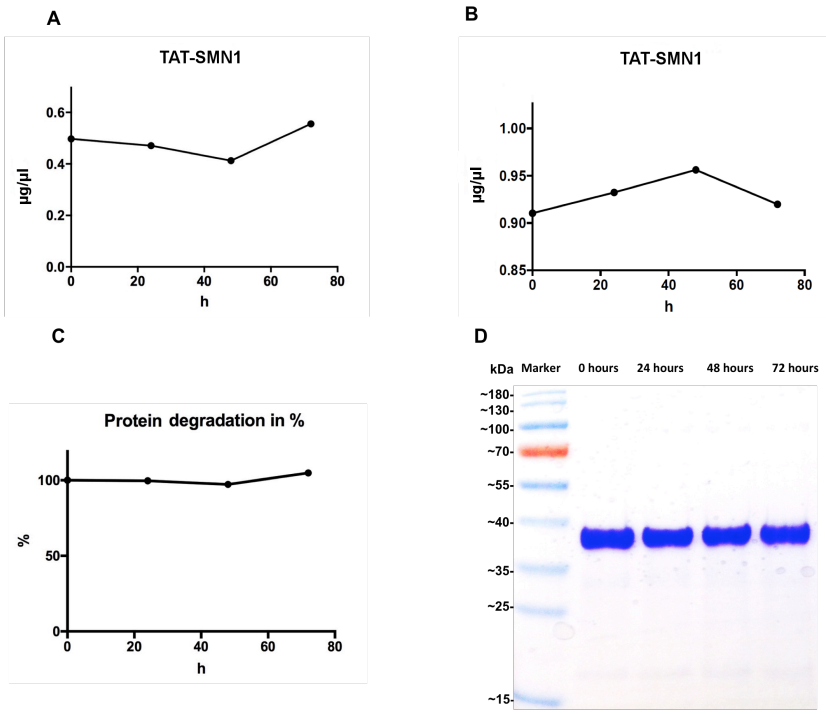

Figure 22: TAT-SMN1 degradation at different time points. A: TAT-SMN1 concentration at different time points (0 hours, 24 hours, 48 hours and 72 hours). The concentration varies from 0.4 µg/µl to 0.6 µg/µl. **B:** TAT-SMN1 concentration at different time points (0 hours, 24 hours, 48 hours and 72 hours). The concentration varies from 0.91 µg/µl to 0.96 µg/µl. **C:** TAT-SMN1 degradation in percentage at different time points. Summary of the results from Figure 22A and 22B. D: 10% SDS Page. Coomassie stain.

4.4. Cell proliferation of NIH3T3 cells after treatment with different TAT-SMN1 concentrations

Cell proliferation was measured using EZ4U - Cell Proliferation Assay. The 125 nM concentration seems to have almost no effect on cell proliferation. The other concentrations have a slight cytotoxic effect **(Figure 23)**.

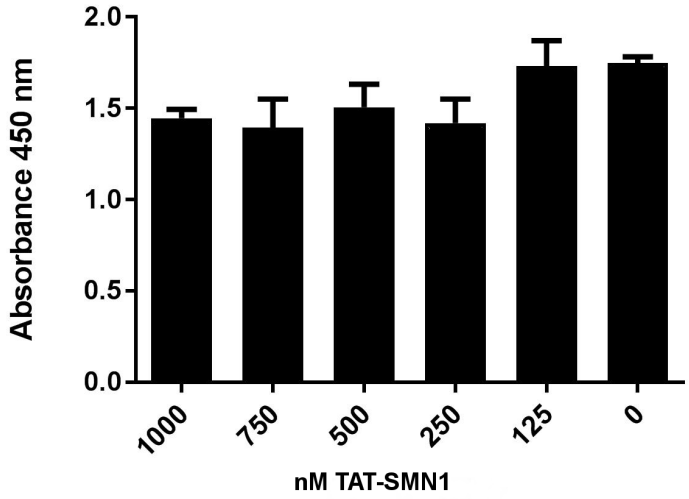

Figure 23: Cell proliferation of NIH3T3 cells after treatment with different TAT-SMN1 concentrations. NIH3T3 cells were treated with different TAT-SMN1 concentrations (0 nM control, 125 nM, 250 nM, 500 nM, 750 nM and 1000 nM). Absorbance was measured at 450 nm.

4.5. Cloning of vector without TAT sequence

A PCR-product was generated from pJexpress411:64109 - TAT_SMN1_Strep_MOD (4913 bp) with Pfu-Polymerase. The blunt-end 942 bp PCR-product was cloned into a previously with EcoRV cut pBluescriptVector, resulting in the pBlueNcoI_BsrGI. pBlueNcoI_BsrGI and pET28_HisTAT_SMN1_Strep were digested with NcoI and BsrGI. The 924 bp fragment from pBlueNcoI_BsrGI and the 5,257 bp fragment from pET28_HisTAT_SMN1_Strep were extracted and ligated to pET28_His_SMN1_Strep (6181 bp). The pET28_His_SMN1_Strep was sequenced using the primers pET28_F1seq, pET28R1, T7.

A PCR product without the TAT sequence was generated using PFU-Polymerase. pBluescript vector was digested using EcoRV. The entire digestion product was loaded on an agarose gel, and DNA was extracted using QI Aquick Gel Extraction Kit (QI Agen). The vector and insert were ligated using T4 ligase and EcoRV. The ligated vector was transformed into One Shot Top 10 cells and plated and LB-AMP + X-Gal plates. The white colonies were used for overnight cultures. The DNA was isolated using DNA Extraction Kit.

To test which sample should be used for further experiments, a control digest was performed using different restriction enzymes:

1) NcoI-HF + BsrG1 (the expected fragments: 924 bp and 3026 bp long)
2) SaII-HF + Eag-HF (the expected fragments: 1006 and 2944 bp long)
3) NdeI + SacI-HF (the expected fragments: 990 bp and 2960 bp long)

The pBlueNcoI_BsrGI Vector is 3950 bp long.

Sample #3 was used for future experiments. The digest with NcoI-HF and BsrG1 seems to have worked for all five samples. Cutting with SaII-HF and Eag-HF led to the expected result in only Samples 1 and 3. The band at approximately 4000 bp is probably the undigested vector indicating that the digest did not completely work. The digest with NdeI and SacI-HF did not lead to the expected results for any of the samples. The band at approximately 4000 bp is probably the undigested vector **(Figure 24)**.

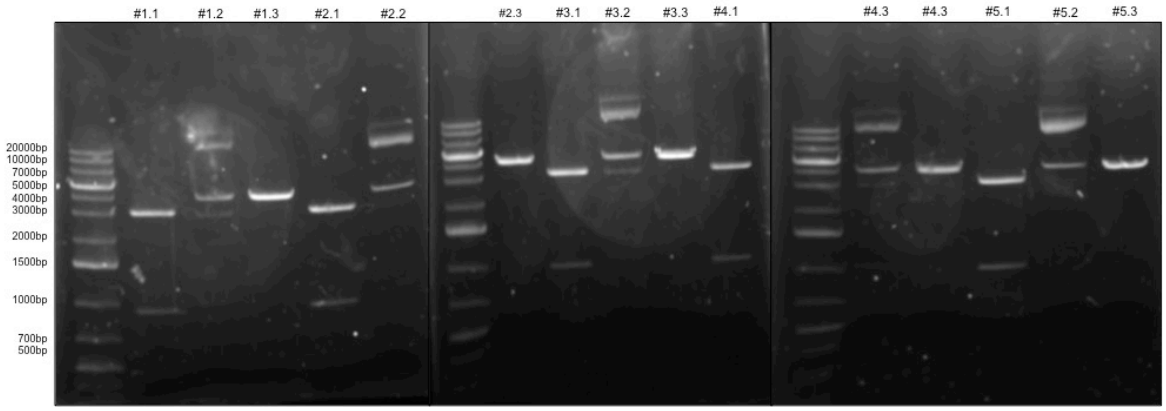

Figure 24: Control digest of pBlueNcoI_BsrGI vector. Samples #1–5 cut with different restriction enzymes. #1.1: Digested with NcoI-HF + BsrG1, a 924 bp and 3026 bp can be seen. #1.2: SaII-HF + Eag-HF: The 2,944 bp fragment can be seen, but the 1006 bp fragment is almost invisible. There is also a fragment at 4000 bp. #1.3: Only one fragment at approximately 4000 bp. #2.1: digested with NcoI-HF + BsrG1, a 924 bp and 3026 bp can be seen. #2.2: The 2,944 bp fragment can be seen, but no 1,006 bp fragment. #2.3: Only one band at approximately 4500 bp. #3.1: 1.1: digested with NcoI-HF + BsrG1, a 924 bp and 3,026 bp can be seen. #3.2: SaII-HF + Eag-HF: The 2,944 bp fragment can be seen, and a very light band at 1006 bp. #3.3: strong band at approximately 5000 bp. (probably the undigested vector.) #4.1: digested with NcoI-HF + BsrG1, a 924 bp and 3,026 bp can be seen. #4.2: SaII-HF + Eag-HF: The 2,944 bp fragment is almost invisible, and no band at 1006 bp.. #4.3: One band at approximately 4000 bp. #5.1: digested with NcoI-HF + BsrG1, a 924 bp and 3026 bp can be seen. #5.2: One band at approximately 4000 bp. #5.3: One band at approximately 4000 bp.

The pBluescript vector with insert and the original vector were both cut with BsrGI and NcoI and loaded on an agarose gel. The 924 bp insert and the 5257 vector were cut out of the gel, and the DNA was isolated **(Figure 25).**

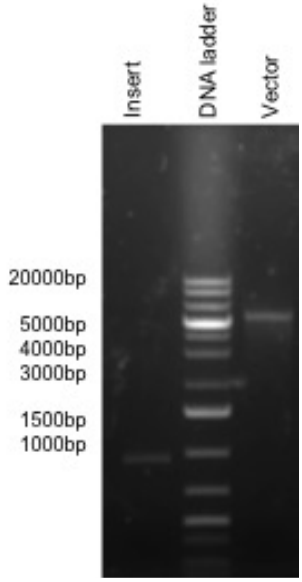

Figure 25: Insert and Vector. Band at 924 bp for Insert and 5,257 bp for Vector.

The insert and the vector were ligated using T4 DNA Ligase. The ligation was transformed into One Shot Top 10 cells. A PCR was performed using the ligation, vector, insert and a control. The PCR products were loaded on a 1% agarose gel. There should only be a PCR product for the ligation **(Figure 26).**

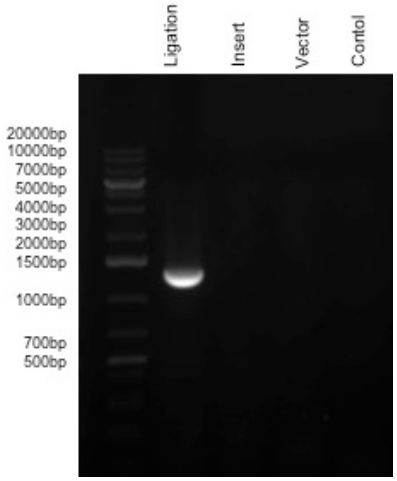

Figure 26: PCR product ligation, vector, insert and a control. Ligation 2: PCR product of ligated insert and vector. Insert: PCR of insert only, no band as expected. Vector PCR of Vector only, no band as expected. Control: negative control.

5. Discussion

SMA is a severe disease brought about by mutations in the SMN1 gene which in turn leads to reduced SMN1 protein levels in the spinal cord. This decrease causes a motor neuron loss. Whereas is no cure for this debilitating and often fatal disease, different therapeutic options are being explored. One such option lies in restoring the SMN1 levels in diseased individuals. Studies have shown that restoration of SMN1 levels leads to an alleviation of disease characteristics (Dominguez et al., 2011). In this study we sought to purify a previously expressed TAT-SMN1 fusion protein that would enter the cell and cell nuclei as form of treatment.

5.1. TAT-SMN1 purification

One of the main aims of this study was to develop a robust protocol for TAT-SMN1 purification. The purification of affinity tagged proteins is a frequently used method. The polyhistidine tag can be purified via metal-chelate chromatography resins (LaVallie & McCoy, 1995). HIS-tag affinity chromatography was used to purify the HIS tagged protein.

When *E. coli* is used for protein overexpression, the proteins sometimes form so-called inclusion bodies. Inclusion bodies are cytoplasmic aggregates. Chaotropic salts or detergents are used for protein extraction from inclusion bodies. Removing the chaotropic salt or detergent will lead to refolding of protein (Bonner, 2007). Refolding is not a straightforward process, aggregation and misfolding can result in an inactive protein (Tsumoto et al., 2003) . However, the fact that *E. coli* expressed proteins build inclusion bodies can be beneficial for protein purification, resulting from the fact that inclusion bodies are homogenous (Fink, 1998).

We used an 8M Urea lysis buffer in our purification process. After HIS-Tag purification, we observed a strong band at approximately 38 kDa when the samples were analyzed by SDS-PAGE **(Figure 7A)**. After the protein was purified using immobilized metal affinity chromatography (IMAC), we aimed to exchange the urea containing buffer.

Buffer-exchange via a PD-10 column *"forces the protein to rapidly hides it's hydrophobic residues and become aqueously soluble"* (Becker-Hapak et al., 2001). We evaluated two different buffers for the PD-10 desalting column. Using 200 mM Tris-HCl, 200 mM NaCl, 10% glycerol, pH=7 leads to higher protein yields compared to 200 mM Tris/HCl, 10%

glycerol and 0.1 mM EDTA, pH=7 **(Figure 7B)**. This was even more apparent after pooling the protein containing fractions and their concentration in a 10000 MWCO **(Figure 7C).**

We used *E. coli* to express the recombinant protein. As *E. coli* is a gram-negative bacterium, it carries endotoxin (a LPS, lipopolysacharid) on its cell wall. Endotoxins can cause a septic shock or inflammation in mammalian hosts. Lipopolysaccharide can also have an effect on cells or cell-free system. This effect makes endotoxin removal from biological products important (S. Liu et al., 1997). For some proteins, the common purification protocols are sufficient for endotoxin removal, while for others, special treatment is necessary (Petsch & Anspach, 2000). In our first experiments, we also attempted for endotoxin removal via an Endotrap column. Unfortunately, that approach led to a loss of a great amount of protein **(Figure 8)**. This loss is most probably due to protein sticking to the Endotrap removal column. This study conducted short-term experiments in cultured cells with TAT-SMN1, so that endotoxicity was taken not a consideration. However, for further analysis, a proper protocol for endotoxin removal should be established. There is no real explanation for the protein loss.

5.2. TAT-SMN1

An important factor that was tested is whether the protein is stable over a certain time period. Protein stability experiments revealed that the protein concentration remains largely stable, with only a slight decrease in concentration over 72 hours. The increase in protein concentration is best explained by evaporation. Percentage-wise, almost no protein degradation is observed. The SDS-PAGE analysis has further confirmed this result **(Figure 23)**. If the fusion protein does not fulfill the expected function, the protein half-life should be investigated. Protein degradation at various time points should be tested (Becker-Hapak et al., 2001). If the protein is to be used for therapeutic measurements, the cellular half-life of the protein has to be determined, so that a proper protocol for treatment can be established.

Another factor that was considered was whether TAT-SMN1 has a negative influence on cell proliferation. One of the main advantages of TAT-mediated protein in delivery is that TAT shows almost no cytotoxicity. A study showed that concentrations of up to 5 mg/ml TAT had no cytotoxic effect on A549-luc-C8 (Baoum et al., 2012). We performed a cell proliferation cytotoxicity test with TAT-SMN1 and NIH3T3 cells. We used the EZ4U assay. The cell proliferation assay revealed that TAT-SMN1 has almost no or only a slight effect on cell proliferation. The treatment with 125 nM of TAT-SMN1 shows no cytotoxic effect, whereas

the 250 nM, 500 nM, 750 nM and 1000 nM treatments have influenced cell proliferation only slightly **(Figure 24)**. These results are consistent with findings that TAT proteins have almost no toxic effect. This experiment indicates that the fusion protein TAT-SMN1 shows almost no cytotoxicity.

SMN1 is localized in the cytoplasm and the nucleus (Lefebvre et al., 1997; Q. Liu et al., 1996). In order for a comprehensive restoration of SMN1 levels to take place, the recombinant protein has to be able to cross the cell wall and to enter the cytoplasm nucleus to. We tested whether our purified protein enters the cell upon treatment. First, in order to get rid of protein that only sticks to the outside of the cell membrane and that could lead to a false positive signal, we treated the NIH3T3 cells with trypsin before fixation. A concentration of 0.0005% trypsin proved most suitable. Transduction of the cell and detection with the anti-His tag antibody led to a certain amount of unspecific binding. For further experiments, we used an anti-Strep tag antibody. Transduction of NIH3T3 cells with 500 nM TAT-SMN1 showed that a small amount of the protein is in the nucleus. The greater amount of the protein is localized around the nucleus in the cytoplasm **(Figure 12).** The SMN protein forms a complex with gemin proteins. Gemin3 is known to be a part of the SMN complex (Pellizzoni, 2007). Co-staining of SMN and Gemin3 led to a strong signal for gemin3. Gemin3 is localized in the nucleus and through the cell. In this case, it is difficult to make an assumption for TAT-SMN1. A small amount of TAT- SMN1 seems to be in the cytoplasm and cell nuclei **(Figure 13).**

In the next experiment we co-stained SMN with an anti-SMN2 antibody and TAT-SMN1 with an anti-Strep antibody. Co-staining indicated that both proteins colocalize in the nucleus and in the cytoplasm **(Figure 14).**

To examine our hypothesis from a different perspective, we decided to perform a Western blot on lysates of previously TAT-SMN1 treated cells. The first step was testing for different antibodies, where STREB MAB Classic conjugated to horseradish peroxidase (1:1000from IBA, #1509-007) proved most suitable. Two different sets of experiments were performed, time-dependent and concentration-dependent. Western blot analysis shows that TAT-SMN1 is in the cell lysates of previously treated NIH3T3 cells. In order to avoid a false positive signal, the media was treated with trypsin, and before that the supernatant media was collected. After trypsinisation and stopping the reaction, the media was collected again. The expected result was that there is a TAT-SMN1 signal in the lysates and in the control that was collected before the protein was degraded by trypsin. The first concentration-dependent experiments were performed without tubulin as a loading control. Nagahara et al., showed that TAT-

p27WT–FITC transduced into the cells in a concentration dependent manner (Nagahara et al., 1998). Based on our experiments, we cannot confirm that TAT-SMN1 transduces in a concentration dependent manner. The next set of experiments was performed in a time dependent manner. As for the time dependence of TAT-SMN1, we showed that a small amount of the protein is taken up by the cell in a timeframe of 15–30 minutes.

This finding agrees with those of Schwarze et al. that TAT-ß-galactosidase transduces into the cell in less than 15 minutes (Schwarze et al., 1999). After this period, a certain amount of TAT-SMN1 remains outside the cell. It is also shown that even after 24 hours, not all of TAT-SMN1 transduced into the cell.

NIH3T3 cells are fibroblast cells. SMA is a neurodegenerative disease. NIH3T3 is not the most suitable cell line for testing. In the next step we decided to use NSC-34 cells: “These cells express many properties of motor neurons, including choline acetyltransferase, ACh synthesis, storage and release and neurofilament triplet proteins” (Cellutions-Biosystems-INC). However, in the first experiments, we observed that NSC-34 cells call for a different handling and an adjusted protocol.

Studies showed that the TAT sequence enables a protein to cross the cell membrane. Recombinant TAT proteins have been shown to cross the cell membranes of different cell types (Fawell et al., 1994). In their study, Schwarze et al. showed that TAT- β-gal transduced into cells. The control protein β-gal did not enter the cell (Schwarze et al., 1999). We have tested the ability of previously purified TAT-SMN1 to enter the cells. In order to demonstrate the effect of the TAT sequence, we aimed to design a vector construct that contains the sequence for SMN1 but without the TAT sequence. We wanted to purify the protein and test protein transduction into the cell. Unfortunately, the sequenced vector showed a base pair exchange, which may have occurred due to a base pair exchange in the sequence. One way to explain the base pair exchange is as a PCR artifact. The PCR program should be investigated and evaluated. Mispriming might be the reason for this. The original vector should be sequenced to see if the base pair exchange is due to a wrong sequence in the original vector.

There is still no cure for SMA. Restoring SMN levels in motor neurons is a promising approach to rescue patients from a severe phenotype functional loss, yet the therapeutic window for treatment is found to be short, and it is important for patients to have access to a therapy as soon as possible. In this study, we have purified the previously expressed TAT-SMN1 protein and shown that this fusion protein is able to cross the cell membrane of NIH3T3 cells. We have further observed that this protein is stable for over 72 hours and that it has almost no cytotoxic effect. Future experiments should concentrate on NSC-34 cells, as

they are the better cell model for SMA. Further, Western Blot analysis of sub-cellular fractionated samples could help to locate TAT-SMN1 in the nuclei of cells. TAT-mediated delivery of the SMN protein is poorly understood, and further testing will reveal whether it is a promising method for SMA therapy.

6. Appendix

6.1. Abbreviations and acronyms

AAV	Adeno-associated virus
ACh	Acetylcholine
α-COP	α-coat protein
ALS	Amyotrophic lateral sclerosis
APS	Ammonium persulfate
ASO	Antisense oligonucleotide
ATP	Adenosintriphosphat
BBB	Blood-brain barrier
BCA	Bicinchoninic acid
BSA	Bovine serum albumin
CARM	Co-activator associated arginine methyltransferase
CNS	Central nervous system
DAPI	4,6-Diamidin-2-phenylindol
DMEM	Dulbecco's modified Eagle's medium
DMSO	Dimethyl sulfoxide
DNA	Deoxyribonucleic acid
EDTA	Ethylenediaminetetraacetic acid
EGTA	Egtazic acid
EPP	Endplate potential
FDA	United States Food and Drug Administration
GFP	Green fluorescence protein
GLT	Glutamate transporter
HDAC	Histone deacetylase
HIV	Human immunodeficiency virus
hnTBP-R	Heterogeneous nuclear ribonucleoprotein R
IPTG	Isopropyl-β-D-thiogalactoside
LB	Lysogeny broth
LTR	Long terminal repeat
KCl	Potassium chloride
MAB	Monoclonal antibody

mRNA	Messenger RNA
NAIP	Neuronal apoptosis inhibitory protein
NHP	Nonhuman primate
NMJ	Neuromuscular junctions
PBS	Phosphate-buffered saline
PCR	Polymerase chain reaction
PGK	Phosphoglycerate kinase
PMSF	Phenylmethylsulfonyl fluoride
PTD	Protein transduction domain
RhoA	Ras homolog gene family, member A
RNP	Ribonucleoprotein
ROCK	Rho-associated, coiled-coil containing protein kinase
SDS	Sodium dodecylsulfate
SDS-PAGE	Sodium dodecyl sulfate polyacrylamide gel electrophoresis
SMA	Spinal muscular atrophy
SMN	Survival motor neuron
siRNA	Small interfering RNA
snRNP	Small nuclear ribonucleoprotein
STS	Staurosporin
TBE	Tris/Borate/EDTA
TAT	Trans-activating transcriptional activator
TAR	Transactivation response element
TEMED	N,N,N',N'-Tetramethyl ethylenediamine
TSPO	Translocator protein
unrip	Unr-interacting protein
VDAC	Voltage-dependent anion channel\
VPA	Valproic acid.
WB	Western Blot

6.2. Abstract

Spinal muscular atrophy (SMA) is a severe autosomal recessive disease with a carrier frequency of 1:40–1:60 that affects 1 in 10.000 live births. SMA is caused by either deletions or mutations within the *survival motor neuron 1 (SMN1)* gene. This sort of changes leads to decreased levels of full-length SMN protein, resulting in a loss of alpha-motor neurons in the spinal cord that leads to atrophy and weakness of limb and trunk muscles. The disease is categorized into four groups, depending on age of onset and severity. Currently, there is no cure for SMA. Different therapeutic strategies are under investigation. One approach involves restoring SMN to physiological concentrations in motor neurons. This should lead to a rescue of the phenotype. Trans-activating transcriptional activator (TAT) has been shown to cross the cell membrane and the blood-brain barrier (BBB). In this study, we aimed to establish a protocol for purification of a previously expressed TAT-SMN1 fusion protein. We were able to show that the protein is stable for over 72 hours and has almost no cytotoxic effect on NIH3T3 cells. We tested TAT-SMN1's ability to cross cell membranes and enter the cytoplasm and cell nuclei. Immunodetection has indicated that upon treatment of NIH3T3 cells with TAT-SMN1, the protein can be localized within cells and their nuclei. Western blot analysis of TAT-SMN1 previously treated with lysates confirmed this result. Our observations serve as a promising basis for further experiments in other cell types and for *in vivo* experiments in the future.

6.3. Zusammenfassung

Die spinale Muskelatrophie (SMA) ist eine schwerwiegende, autosomal-rezessiv vererbte neurodegenerative Erkrankung mit einer Trägerwahrscheinlichkeit von 1:40–1:60. Die Erkrankung betrifft eine von 10.000 Lebendgeburten pro Jahr. Spinale Muskelatrophie wird durch die Deletion des *survival motor neuron 1 (SMN1)* Gens bzw. durch eine Mutation desselben verursacht. Dadurch kommt es zur Verminderung der SMN1-Proteinmenge, der sich im Verlust von Alpha-Motorneuronen im Rückenmark äußert. Dieser Verlust führt zu einer Schwäche der Glieder- und Rumpfmuskulatur. Die Krankheit wird in vier Gruppen untergliedert, die vom Schweregrad und dem Ausbruchsalter abhängen. Unterschiedliche therapeutische Maßnahmen werden derzeit untersucht, aber bis jetzt gibt es noch keine Heilung von SMA. Einer der bedeutendsten Ansätze liegt in der Erhöhung der SMN1-Proteinmenge in den Motorneuronen, sodass diese wieder auf das Niveau eines Gesunden angeglichen wird. Es konnte gezeigt werden, dass das zellpenetrierende Peptid TAT (trans-activating transcriptional activator) die Zellmembran, wie auch die Blut-Hirn-Schranke passieren kann. In dieser Forschungsarbeit wurde ein Protokoll zur Aufreinigung von TAT-SMN1, einem Fusionsprotein, erstellt. Wir konnten aufzeigen, dass das Protein über einen Zeitraum von 72 Stunden stabil ist und dass es keinen zytotoxischen Auswirkungen auf NIH3T3-Zellen hatte. Wir untersuchten die Fähigkeit des Proteins, die Zellmembran zu passieren und in die Zelle bzw. den Zellkern einzutreten. Dies wurde mithilfe von Westernblot-Versuchen bestätigt. Unsere Resultate bilden eine vielversprechende Basis für weitere Versuche an anderen Zelltypen bzw. für *in-vivo* Versuche in der Zukunft.

7. References

Akutsu, T., Nishio, H., Sumino, K., Takeshima, Y., Tsuneishi, S., Wada, H., Takada, S., Matsuo, M., & Nakamura, H. (2002). Molecular genetics of spinal muscular atrophy: contribution of the NAIP gene to clinical severity. *Kobe J Med Sci, 48*(1-2), 25-31.

Andermann, A., Blancquaert, I., Beauchamp, S., & Déry, V. (2008). Revisiting Wilson and Jungner in the genomic age: a review of screening criteria over the past 40 years. *Bull World Health Organ, 86*(4), 317-319. doi:10.2471/blt.07.050112

Azzouz, M., Le, T., Ralph, G. S., Walmsley, L., Monani, U. R., Lee, D. C. P., Wilkes, F., Mitrophanous, K. A., Kingsman, S. M., Burghes, A. H. M., & Mazarakis, N. D. (2004). Lentivector-mediated SMN replacement in a mouse model of spinal muscular atrophy. *The Journal of Clinical Investigation, 114*(12), 1726-1731. doi:10.1172/JCI22922

Baoum, A., Ovcharenko, D., & Berkland, C. (2012). Calcium condensed cell penetrating peptide complexes offer highly efficient, low toxicity gene silencing. *International Journal of Pharmaceutics, 427*(1), 134-142. doi:https://doi.org/10.1016/j.ijpharm.2011.08.012

Becker-Hapak, M., McAllister, S. S., & Dowdy, S. F. (2001). TAT-mediated protein transduction into mammalian cells. *Methods, 24*(3), 247-256. doi:10.1006/meth.2001.1186

Boffa, L. C., Vidali, G., Mann, R. S., & Allfrey, V. G. (1978). Suppression of histone deacetylation in vivo and in vitro by sodium butyrate. *Journal of Biological Chemistry, 253*(10), 3364-3366.

Bonner, P. L. R. (2007). *Protein Purification*: Taylor & Francis.

Bordet, T., Buisson, B., Michaud, M., Drouot, C., Galea, P., Delaage, P., Akentieva, N. P., Evers, A. S., Covey, D. F., & Ostuni, M. A. (2007). Identification and characterization of cholest-4-en-3-one, oxime (TRO19622), a novel drug candidate for amyotrophic lateral sclerosis. *Journal of Pharmacology and Experimental Therapeutics, 322*(2), 709-720.

Bowerman, M., Beauvais, A., Anderson, C. L., & Kothary, R. (2010). Rho-kinase inactivation prolongs survival of an intermediate SMA mouse model. *Hum Mol Genet, 19*(8), 1468-1478. doi:10.1093/hmg/ddq021

Bowerman, M., Michalski, J.-P., Beauvais, A., Murray, L. M., DeRepentigny, Y., & Kothary, R. (2014). Defects in pancreatic development and glucose metabolism in SMN-depleted mice independent of canonical spinal muscular atrophy neuromuscular pathology. *Hum Mol Genet, 23*(13), 3432-3444. doi:10.1093/hmg/ddu052

Bowerman, M., Swoboda, K. J., Michalski, J.-P., Wang, G.-S., Reeks, C., Beauvais, A., Murphy, K., Woulfe, J., Screaton, R. A., Scott, F. W., & Kothary, R. (2012). Glucose metabolism and pancreatic defects in spinal muscular atrophy. *Annals of Neurology, 72*(2), 256-268. doi:10.1002/ana.23582

Brichta, L., Hofmann, Y., Hahnen, E., Siebzehnrubl, F., Raschke, H., Blumcke, I., Eyupoglu, I., & Wirth, B. (2003). Valproic acid increases the SMN2 protein level: a well-known drug as a potential therapy for spinal muscular atrophy. *Hum Mol Genet, 12*(19), 2481-2489.

Butchbach, M. E. R., Rose, F. F., Rhoades, S., Marston, J., McCrone, J. T., Sinnott, R., & Lorson, C. L. (2010). Effect of diet on the survival and phenotype of a mouse

model for spinal muscular atrophy. *Biochemical and Biophysical Research Communications, 391*(1), 835-840. doi:https://doi.org/10.1016/j.bbrc.2009.11.148
Campbell, L., Potter, A., Ignatius, J., Dubowitz, V., & Davies, K. (1997). Genomic Variation and Gene Conversion in Spinal Muscular Atrophy: Implications for Disease Process and Clinical Phenotype. *The American Journal of Human Genetics, 61*(1), 40-50. doi:https://doi.org/10.1086/513886
Cao, G., Pei, W., Ge, H., Liang, Q., Luo, Y., Sharp, F. R., Lu, A., Ran, R., Graham, S. H., & Chen, J. (2002). In Vivo Delivery of a Bcl-xL Fusion Protein Containing the TAT Protein Transduction Domain Protects against Ischemic Brain Injury and Neuronal Apoptosis. *J Neurosci, 22*(13), 5423-5431. doi:20026550
Carissimi, C., Baccon, J., Straccia, M., Chiarella, P., Maiolica, A., Sawyer, A., Rappsilber, J., & Pellizzoni, L. (2005). Unrip is a component of SMN complexes active in snRNP assembly. *FEBS Letters, 579*(11), 2348-2354. doi:10.1016/j.febslet.2005.03.034
Cellutions-Biosystems-INC. Mouse Motor Neuron (NSC-34) Cell Line Maintenance.
Chang, J.-G., Hsieh-Li, H.-M., Jong, Y.-J., Wang, N. M., Tsai, C.-H., & Li, H. (2001). Treatment of spinal muscular atrophy by sodium butyrate. *Proc Natl Acad Sci U S A, 98*(17), 9808-9813. doi:10.1073/pnas.171105098
Chen, W. J., Dong, W. J., Lin, X. Z., Lin, M. T., Murong, S. X., Wu, Z. Y., & Wang, N. (2009). Rapid diagnosis of spinal muscular atrophy using High-Resolution Melting Analysis. *BMC Medical Genetics, 10*(1), 45. doi:10.1186/1471-2350-10-45
Cho, S., & Dreyfuss, G. (2010). A degron created by SMN2 exon 7 skipping is a principal contributor to spinal muscular atrophy severity. *Genes Dev, 24*(5), 438-442. doi:10.1101/gad.1884910
Corey, D. R. (2017). Nusinersen, an antisense oligonucleotide drug for spinal muscular atrophy. *Nature Neuroscience, 20*, 497. doi:10.1038/nn.4508
Corti, S., Nizzardo, M., Nardini, M., Donadoni, C., Salani, S., Ronchi, D., Saladino, F., Bordoni, A., Fortunato, F., Del Bo, R., Papadimitriou, D., Locatelli, F., Menozzi, G., Strazzer, S., Bresolin, N., & Comi, G. P. (2008). Neural stem cell transplantation can ameliorate the phenotype of a mouse model of spinal muscular atrophy. *The Journal of Clinical Investigation, 118*(10), 3316-3330. doi:10.1172/JCI35432
Deschenes, M. R., Maresh, C. M., & Kraemer, W. J. (1994). The Neuromuscular Junction: Structure, Function, and its Role in the Excitation of Muscle. *The Journal of Strength & Conditioning Research, 8*(2), 103-109.
Dessaud, E., André, C., Scherrer, B., Berna, P., Pruss, R., Cuvier, V., Hauke, W., Bruno, C., Chabrol, B., Comi, G., Cuisset, J. M., Deconinck, N., Goemans, N., Estournet, B., Fontaine-Carbonel, S., Gorni, K., Kirschner, J., Lusakowska, A., Lochmuller, H., Mayer, M., Mercuri, E., Müller-Felber, W., Muntoni, F., Rivier, F., Roper, H., Schara, U., den Berg, L. V., Vita, G., Walter, M., & Bertini, E. (2014). G.O.19: Results of a phase II study to assess safety and efficacy of olesoxime (TRO19622) in 3–25 years old spinal muscular atrophy patients. *Neuromuscular Disorders, 24*(9), 920-921. doi:https://doi.org/10.1016/j.nmd.2014.06.418
Dominguez, E., Marais, T., Chatauret, N., Benkhelifa-Ziyyat, S., Duque, S., Ravassard, P., Carcenac, R., Astord, S., de Moura, A. P., Voit, T., & Barkats, M. (2011). Intravenous scAAV9 delivery of a codon-optimized SMN1 sequence rescues SMA mice. *Hum Mol Genet, 20*(4), 681-693. doi:10.1093/hmg/ddq514
Dubowitz, V. (1999). Very severe spinal muscular atrophy (SMA type 0): an expanding clinical phenotype. *European Journal of Paediatric Neurology, 3*(2), 49-51. doi:https://doi.org/10.1016/S1090-3798(99)80012-9

Fan, L., & Simard, L. R. (2002). Survival motor neuron (SMN) protein: role in neurite outgrowth and neuromuscular maturation during neuronal differentiation and development. *Hum Mol Genet, 11*(14), 1605-1614.
Fawell, S., Seery, J., Daikh, Y., Moore, C., Chen, L. L., Pepinsky, B., & Barsoum, J. (1994). Tat-mediated delivery of heterologous proteins into cells. *Proc Natl Acad Sci U S A, 91*(2), 664-668.
Feldkötter, M., Schwarzer, V., Wirth, R., Wienker, T. F., & Wirth, B. (2002). Quantitative Analyses of SMN1 and SMN2 Based on Real-Time LightCycler PCR: Fast and Highly Reliable Carrier Testing and Prediction of Severity of Spinal Muscular Atrophy. *The American Journal of Human Genetics, 70*(2), 358-368. doi:https://doi.org/10.1086/338627
Fink, A. L. (1998). Protein aggregation: folding aggregates, inclusion bodies and amyloid. *Folding and Design, 3*(1), R9-R23. doi:https://doi.org/10.1016/S1359-0278(98)00002-9
Fischer, U., Liu, Q., & Dreyfuss, G. The SMN–SIP1 Complex Has an Essential Role in Spliceosomal snRNP Biogenesis. *Cell, 90*(6), 1023-1029. doi:10.1016/S0092-8674(00)80368-2
Foust, K. D., Wang, X., McGovern, V. L., Braun, L., Bevan, A. K., Haidet, A. M., Le, T. T., Morales, P. R., Rich, M. M., Burghes, A. H. M., & Kaspar, B. K. (2010). Rescue of the spinal muscular atrophy phenotype in a mouse model by early postnatal delivery of SMN. *Nature Biotechnology, 28*, 271. doi:10.1038/nbt.1610
https://www.nature.com/articles/nbt.1610 - supplementary-information
Frankel, A. D., & Pabo, C. O. (1988). Cellular uptake of the tat protein from human immunodeficiency virus. *Cell, 55*(6), 1189-1193.
Gabanella, F., Butchbach, M. E., Saieva, L., Carissimi, C., Burghes, A. H., & Pellizzoni, L. (2007). Ribonucleoprotein assembly defects correlate with spinal muscular atrophy severity and preferentially affect a subset of spliceosomal snRNPs. *PloS one, 2*(9), e921.
Green, M., & Loewenstein, P. M. (1988). Autonomous functional domains of chemically synthesized human immunodeficiency virus tat trans-activator protein. *Cell, 55*(6), 1179-1188.
Grzeschik, S. M., Ganta, M., Prior, T. W., Heavlin, W. D., & Wang, C. H. (2005). Hydroxyurea enhances SMN2 gene expression in spinal muscular atrophy cells. *Annals of Neurology, 58*(2), 194-202. doi:10.1002/ana.20548
Gubitz, A. K., Feng, W., & Dreyfuss, G. (2004). The SMN complex. *Experimental Cell Research, 296*(1), 51-56. doi:https://doi.org/10.1016/j.yexcr.2004.03.022
Hamilton, G., & Gillingwater, T. H. (2013). Spinal muscular atrophy: going beyond the motor neuron. *Trends in Molecular Medicine, 19*(1), 40-50. doi:https://doi.org/10.1016/j.molmed.2012.11.002
Heath, P. R., & Shaw, P. J. (2002). Update on the glutamatergic neurotransmitter system and the role of excitotoxicity in amyotrophic lateral sclerosis. *Muscle & Nerve, 26*(4), 438-458. doi:10.1002/mus.10186
Hinderer, C., Katz, N., Buza, E. L., Dyer, C., Goode, T., Bell, P., Richman, L., & Wilson, J. M. (2018). Severe toxicity in nonhuman primates and piglets following high-dose intravenous administration of an AAV vector expressing human SMN. *Human gene therapy*(ja).
Hofmann, Y., Lorson, C. L., Stamm, S., Androphy, E. J., & Wirth, B. (2000). Htra2-β1 stimulates an exonic splicing enhancer and can restore full-length SMN expression to survival motor neuron 2 (SMN2). *Proceedings of the National Academy of Sciences, 97*(17), 9618-9623.

Jedrzejowska, M., Milewski, M., Zimowski, J., Borkowska, J., Kostera-Pruszczyk, A., Sielska, D., Jurek, M., & Hausmanowa-Petrusewicz, I. (2009). Phenotype modifiers of spinal muscular atrophy: the number of SMN2 gene copies, deletion in the NAIP gene and probably gender influence the course of the disease. *Acta Biochim Pol, 56*(1), 103-108.

Jodelka, F. M., Ebert, A. D., Duelli, D. M., & Hastings, M. L. (2010). A feedback loop regulates splicing of the spinal muscular atrophy-modifying gene, SMN2. *Hum Mol Genet, 19*(24), 4906-4917. doi:10.1093/hmg/ddq425

Kanning, K. C., Kaplan, A., & Henderson, C. E. (2010). Motor Neuron Diversity in Development and Disease. *Annual Review of Neuroscience, 33*(1), 409-440. doi:10.1146/annurev.neuro.051508.135722

Kariya, S., Park, G.-H., Maeno-Hikichi, Y., Leykekhman, O., Lutz, C., Arkovitz, M. S., Landmesser, L. T., & Monani, U. R. (2008). Reduced SMN protein impairs maturation of the neuromuscular junctions in mouse models of spinal muscular atrophy. *Hum Mol Genet, 17*(16), 2552-2569. doi:10.1093/hmg/ddn156

LaVallie, E. R., & McCoy, J. M. (1995). Gene fusion expression systems in Escherichia coli. *Current Opinion in Biotechnology, 6*(5), 501-506. doi:https://doi.org/10.1016/0958-1669(95)80083-2

Lefebvre, S., Bürglen, L., Reboullet, S., Clermont, O., Burlet, P., Viollet, L., Benichou, B., Cruaud, C., Millasseau, P., Zeviani, M., Le Paslier, D., Frézal, J., Cohen, D., Weissenbach, J., Munnich, A., & Melki, J. (1995). Identification and characterization of a spinal muscular atrophy-determining gene. *Cell, 80*(1), 155-165. doi:https://doi.org/10.1016/0092-8674(95)90460-3

Lefebvre, S., Burlet, P., Liu, Q., Bertrandy, S., Clermont, O., Munnich, A., Dreyfuss, G., & Melki, J. (1997). Correlation between severity and SMN protein level in spinal muscular atrophy. *Nature Genetics, 16*, 265. doi:10.1038/ng0797-265

Lewelt, A., Krosschell, K. J., Stoddard, G. J., Weng, C., Xue, M., Marcus, R. L., Gappmaier, E., Viollet, L., Johnson, B. A., White, A. T., Viazzo-Trussell, D., Lopes, P., Lane, R. H., Carey, J. C., & Swoboda, K. J. (2015). Resistance strength training exercise in children with spinal muscular atrophy. *Muscle & Nerve, 52*(4), 559-567. doi:10.1002/mus.24568

Little, S. E., Janakiraman, V., Kaimal, A., Musci, T., Ecker, J., & Caughey, A. B. (2010). The cost-effectiveness of prenatal screening for spinal muscular atrophy. *American Journal of Obstetrics and Gynecology, 202*(3), 253.e251-253.e257. doi:https://doi.org/10.1016/j.ajog.2010.01.032

Liu, Q., & Dreyfuss, G. (1996). A novel nuclear structure containing the survival of motor neurons protein. *Embo j, 15*(14), 3555-3565.

Liu, S., Tobias, R., McClure, S., Styba, G., Shi, Q., & Jackowski, G. (1997). Removal of Endotoxin from Recombinant Protein Preparations. *Clinical Biochemistry, 30*(6), 455-463. doi:https://doi.org/10.1016/S0009-9120(97)00049-0

Lorson, C. L., Hahnen, E., Androphy, E. J., & Wirth, B. (1999). A single nucleotide in the SMN gene regulates splicing and is responsible for spinal muscular atrophy. *Proc Natl Acad Sci U S A, 96*(11), 6307-6311.

Lorson, C. L., Strasswimmer, J., Yao, J.-M., Baleja, J. D., Hahnen, E., Wirth, B., Le, T., Burghes, A. H. M., & Androphy, E. J. (1998). SMN oligomerization defect correlates with spinal muscular atrophy severity. *Nature Genetics, 19*, 63. doi:10.1038/ng0598-63

Louvel, E., Hugon, J., & Doble, A. (1997). Therapeutic advances in amyotrophic lateral sclerosis. *Trends in Pharmacological Sciences, 18*(6), 196-203. doi:https://doi.org/10.1016/S0165-6147(97)01062-6

Macleod, M. J., Taylor, J. E., Lunt, P. W., Mathew, C. G., & Robb, S. A. (1999). Prenatal onset spinal muscular atrophy. *European Journal of Paediatric Neurology, 3*(2), 65-72. doi:https://doi.org/10.1016/S1090-3798(99)80015-4

McCarty, D. M. (2008). Self-complementary AAV Vectors; Advances and Applications. *Molecular Therapy, 16*(10), 1648-1656. doi:https://doi.org/10.1038/mt.2008.171

Monani, U. R. (2005). Spinal Muscular Atrophy: A Deficiency in a Ubiquitous Protein; a Motor Neuron-Specific Disease. *Neuron, 48*(6), 885-895. doi:https://doi.org/10.1016/j.neuron.2005.12.001

Morikawa, S., Harahap, I. S., Kaszynski, R. H., Yamamoto, T., Pramudya, D. K., Pham, H. T., Hartomo, T. B., Lee, M. J., Morioka, I., Nishimura, N., Yokoyama, N., Ueno, Y., Matsuo, M., & Nishio, H. (2011). Diagnosis of spinal muscular atrophy via high-resolution melting analysis symmetric polymerase chain reaction without probe: a screening evaluation for SMN1 deletions and intragenic mutations. *Genet Test Mol Biomarkers, 15*(10), 677-684. doi:10.1089/gtmb.2010.0237

Nagahara, H., Vocero-Akbani, A. M., Snyder, E. L., Ho, A., Latham, D. G., Lissy, N. A., Becker-Hapak, M., Ezhevsky, S. A., & Dowdy, S. F. (1998). Transduction of full-length TAT fusion proteins into mammalian cells: TAT-p27Kip1 induces cell migration. *Nature Medicine, 4*, 1449. doi:10.1038/4042

Nizzardo, M., Nardini, M., Ronchi, D., Salani, S., Donadoni, C., Fortunato, F., Colciago, G., Falcone, M., Simone, C., Riboldi, G., Govoni, A., Bresolin, N., Comi, G. P., & Corti, S. (2011). Beta-lactam antibiotic offers neuroprotection in a spinal muscular atrophy model by multiple mechanisms. *Experimental Neurology, 229*(2), 214-225. doi:https://doi.org/10.1016/j.expneurol.2011.01.017

Nurputra, D. K., Lai, P. S., Harahap, N. I. F., Morikawa, S., Yamamoto, T., Nishimura, N., Kubo, Y., Takeuchi, A., Saito, T., Takeshima, Y., Tohyama, Y., Tay, S. K. H., Low, P. S., Saito, K., & Nishio, H. (2013). Spinal Muscular Atrophy: From Gene Discovery to Clinical Trials. *Annals of Human Genetics, 77*(5), 435-463. doi:10.1111/ahg.12031

Orzalesi, M., & Danhaive, O. (2009). Ethical problems with neonatal screening. *Ann Ist Super Sanita, 45*(3), 325-330.

Passini, M. A., Bu, J., Roskelley, E. M., Richards, A. M., Sardi, S. P., O'Riordan, C. R., Klinger, K. W., Shihabuddin, L. S., & Cheng, S. H. (2010). CNS-targeted gene therapy improves survival and motor function in a mouse model of spinal muscular atrophy. *The Journal of Clinical Investigation, 120*(4), 1253-1264.

Pellizzoni, L. (2007). Chaperoning ribonucleoprotein biogenesis in health and disease. *EMBO reports, 8*(4), 340-345. doi:10.1038/sj.embor.7400941

Pellizzoni, L., Yong, J., & Dreyfuss, G. (2002). Essential Role for the SMN Complex in the Specificity of snRNP Assembly. *Science, 298*(5599), 1775-1779. doi:10.1126/science.1074962

Peter, C. J., Evans, M., Thayanithy, V., Taniguchi-Ishigaki, N., Bach, I., Kolpak, A., Bassell, G. J., Rossoll, W., Lorson, C. L., & Bao, Z.-Z. (2011). The COPI vesicle complex binds and moves with survival motor neuron within axons. *Hum Mol Genet, 20*(9), 1701-1711.

Petsch, D., & Anspach, F. B. (2000). Endotoxin removal from protein solutions. *Journal of Biotechnology, 76*(2), 97-119. doi:https://doi.org/10.1016/S0168-1656(99)00185-6

Prior, T. W. (2008). Carrier screening for spinal muscular atrophy. *Genetics In Medicine, 10*, 840. doi:10.1097/GIM.0b013e318188d069

Prior, T. W., Snyder, P. J., Rink, B. D., Pearl, D. K., Pyatt, R. E., Mihal, D. C., Conlan, T., Schmalz, B., Montgomery, L., Ziegler, K., Noonan, C., Hashimoto, S., & Garner, S. (2010). Newborn and carrier screening for spinal muscular atrophy. *American*

Journal of Medical Genetics Part A, 152A(7), 1608-1616. doi:10.1002/ajmg.a.33474
Richard, J. P., Melikov, K., Brooks, H., Prevot, P., Lebleu, B., & Chernomordik, L. V. (2005). Cellular Uptake of Unconjugated TAT Peptide Involves Clathrin-dependent Endocytosis and Heparan Sulfate Receptors. *Journal of Biological Chemistry, 280*(15), 15300-15306. doi:10.1074/jbc.M401604200
Richard, J. P., Melikov, K., Vives, E., Ramos, C., Verbeure, B., Gait, M. J., Chernomordik, L. V., & Lebleu, B. (2003). Cell-penetrating Peptides: A REEVALUATION OF THE MECHANISM OF CELLULAR UPTAKE. *Journal of Biological Chemistry, 278*(1), 585-590. doi:10.1074/jbc.M209548200
Rossoll, W., Jablonka, S., Andreassi, C., Kröning, A.-K., Karle, K., Monani, U. R., & Sendtner, M. (2003). Smn, the spinal muscular atrophy–determining gene product, modulates axon growth and localization of β-actin mRNA in growth cones of motoneurons. *The Journal of cell biology, 163*(4), 801-812.
Rothstein, J. D., Patel, S., Regan, M. R., Haenggeli, C., Huang, Y. H., Bergles, D. E., Jin, L., Dykes Hoberg, M., Vidensky, S., Chung, D. S., Toan, S. V., Bruijn, L. I., Su, Z.-z., Gupta, P., & Fisher, P. B. (2005). β-Lactam antibiotics offer neuroprotection by increasing glutamate transporter expression. *Nature, 433*, 73. doi:10.1038/nature03180
https://www.nature.com/articles/nature03180 - supplementary-information
Roy, N., Mahadevan, M. S., McLean, M., Shutter, G., Yaraghi, Z., Farahani, R., Baird, S., Besner-Johnston, A., Lefebvre, C., Kang, X., Salih, M., Aubry, H., Tamai, K., Guan, X., Ioannou, P., Crawford, T. O., de Jong, P. J., Surh, L., Ikeda, J.-E., Korneluk, R. G., & MacKenzie, A. (1995). The gene for neuronal apoptosis inhibitory protein is partially deleted in individuals with spinal muscular atrophy. *Cell, 80*(1), 167-178. doi:https://doi.org/10.1016/0092-8674(95)90461-1
Russman, B. S. (2007). Spinal Muscular Atrophy: Clinical Classification and Disease Heterogeneity. *Journal of Child Neurology, 22*(8), 946-951. doi:10.1177/0883073807305673
Russman, B. S., Iannaccone, S. T., & Samaha, F. J. (2003). A phase 1 trial of riluzole in spinal muscular atrophy. *Archives of Neurology, 60*(11), 1601-1603. doi:10.1001/archneur.60.11.1601
Sanchez, G., Dury, A. Y., Murray, L. M., Biondi, O., Tadesse, H., El Fatimy, R., Kothary, R., Charbonnier, F., Khandjian, E. W., & Côté, J. (2013). A novel function for the survival motoneuron protein as a translational regulator. *Hum Mol Genet, 22*(4), 668-684. doi:10.1093/hmg/dds474
Schwarze, S. R., Ho, A., Vocero-Akbani, A., & Dowdy, S. F. (1999). In Vivo Protein Transduction: Delivery of a Biologically Active Protein into the Mouse. *Science, 285*(5433), 1569-1572. doi:10.1126/science.285.5433.1569
Shanmugarajan, S., Swoboda, K. J., Iannaccone, S. T., Ries, W. L., Maria, B. L., & Reddy, S. V. (2007). Congenital Bone Fractures in Spinal Muscular Atrophy: Functional Role for SMN Protein in Bone Remodeling. *Journal of Child Neurology, 22*(8), 967-973. doi:10.1177/0883073807305664
Stifani, N. (2014). Motor neurons and the generation of spinal motor neuron diversity. *Frontiers in Cellular Neuroscience, 8*, 293. doi:10.3389/fncel.2014.00293
Suzuki, T., Futaki, S., Niwa, M., Tanaka, S., Ueda, K., & Sugiura, Y. (2002). Possible Existence of Common Internalization Mechanisms among Arginine-rich Peptides. *Journal of Biological Chemistry, 277*(4), 2437-2443. doi:10.1074/jbc.M110017200
Taylor, J. E., Thomas, N. H., Lewis, C. M., Abbs, S. J., Rodrigues, N. R., Davies, K. E., & Mathew, C. G. (1998). Correlation of SMNt and SMNc gene copy number with age

of onset and survival in spinal muscular atrophy. *European Journal Of Human Genetics, 6*, 467. doi:10.1038/sj.ejhg.5200210
Ting, C.-H., Wen, H.-L., Liu, H.-C., Hsieh-Li, H.-M., Li, H., & Lin-Chao, S. (2012). The spinal muscular atrophy disease protein SMN is linked to the Golgi network. *PloS one, 7*(12), e51826.
Tsumoto, K., Ejima, D., Kumagai, I., & Arakawa, T. (2003). Practical considerations in refolding proteins from inclusion bodies. *Protein Expression and Purification, 28*(1), 1-8. doi:https://doi.org/10.1016/S1046-5928(02)00641-1
van der Steege, G., Grootscholten, P. M., van der Vlies, P., Draaijers, T. G., Osinga, J., Cobben, J. M., Scheffer, H., & Buys, C. H. C. M. (1995). PCR-based DNA test to confirm clinical diagnosis of autosomal recessive spinal muscular atrophy. *The Lancet, 345*(8955), 985-986. doi:https://doi.org/10.1016/S0140-6736(95)90732-7
Verhaart, I. E. C., Robertson, A., Wilson, I. J., Aartsma-Rus, A., Cameron, S., Jones, C. C., Cook, S. F., & Lochmüller, H. (2017). Prevalence, incidence and carrier frequency of 5q–linked spinal muscular atrophy – a literature review. *Orphanet Journal of Rare Diseases, 12*, 124. doi:10.1186/s13023-017-0671-8
Vitte, J., Fassier, C., Tiziano, F. D., Dalard, C., Soave, S., Roblot, N., Brahe, C., Saugier-Veber, P., Bonnefont, J. P., & Melki, J. (2007). Refined Characterization of the Expression and Stability of the SMN Gene Products. *Am J Pathol, 171*(4), 1269-1280. doi:10.2353/ajpath.2007.070399
Vivès, E., Brodin, P., & Lebleu, B. (1997). A Truncated HIV-1 Tat Protein Basic Domain Rapidly Translocates through the Plasma Membrane and Accumulates in the Cell Nucleus. *Journal of Biological Chemistry, 272*(25), 16010-16017. doi:10.1074/jbc.272.25.16010
Wadia, J. S., & Dowdy, S. F. (2002). Protein transduction technology. *Current Opinion in Biotechnology, 13*(1), 52-56. doi:https://doi.org/10.1016/S0958-1669(02)00284-7
Wan, L., Battle, D. J., Yong, J., Gubitz, A. K., Kolb, S. J., Wang, J., & Dreyfuss, G. (2005). The survival of motor neurons protein determines the capacity for snRNP assembly: biochemical deficiency in spinal muscular atrophy. *Molecular and cellular biology, 25*(13), 5543-5551.
Weigel, P. H., & Oka, J. A. (1981). Temperature dependence of endocytosis mediated by the asialoglycoprotein receptor in isolated rat hepatocytes. Evidence for two potentially rate-limiting steps. *Journal of Biological Chemistry, 256*(6), 2615-2617.
Wilson, J. M. G., Jungner, G., & Organization, W. H. (1968). Principles and practice of screening for disease.
Wirth, B., Schmidt, T., Hahnen, E., Rudnik-Schöneborn, S., Krawczak, M., Müller-Myhsok, B., Schönling, J., & Zerres, K. (1997). De Novo Rearrangements Found in 2% of Index Patients with Spinal Muscular Atrophy: Mutational Mechanisms, Parental Origin, Mutation Rate, and Implications for Genetic Counseling. *The American Journal of Human Genetics, 61*(5), 1102-1111. doi:https://doi.org/10.1086/301608
Wolstencroft, E. C., Mattis, V., Bajer, A. A., Young, P. J., & Lorson, C. L. (2005). A non-sequence-specific requirement for SMN protein activity: the role of aminoglycosides in inducing elevated SMN protein levels. *Hum Mol Genet, 14*(9), 1199-1210. doi:10.1093/hmg/ddi131
Zhang, H. L., Pan, F., Hong, D., Shenoy, S. M., Singer, R. H., & Bassell, G. J. (2003). Active transport of the survival motor neuron protein and the role of exon-7 in cytoplasmic localization. *Journal of Neuroscience, 23*(16), 6627-6637.
Zou, L., Peng, Q., Wang, P., & Zhou, B. (2017). Progress in Research and Application of HIV-1 TAT-Derived Cell-Penetrating Peptide. *The Journal of Membrane Biology, 250*(2), 115-122. doi:10.1007/s00232-016-9940-z